ELSEVIER

Polymer 42 (2001) 10155–10180

polymer

www.elsevier.com/locate/polymer

Toughenability of Nylon-6 with $CaCO_3$ filler particles: new findings and general principles

M.W.L. Wilbrink[a,c], A.S. Argon[a,*], R.E. Cohen[d], M. Weinberg[b]

[a]*Department of Mechanical Engineering, Massachusetts Institute of Technology, Cambridge, MA 02139-4307, USA*
[b]*E.I. duPont de Nemours Company, Central Research and Development Department, Experiment Station, Wilmington, DE 19898, USA*
[c]*The Technische Universiteit Eindhoven, Eindhoven, The Netherlands*
[d]*Department of Chemical Engineering, Massachusetts Institute of Technology, Cambridge, MA 02139-4307, USA*

Received 22 February 2001; received in revised form 23 July 2001; accepted 26 July 2001

Abstract

The mechanical behavior of Nylon-6 blends modified by two types of $CaCO_3$ particles of 0.7 and 3.5 μm diameter with particle volume fractions ranging from 0.05 to 0.28 was studied between −30 and 60°C in slow tension, and at 20°C in bending impact. Additional experiments were also carried out at 20°C to determine the plane stress fracture toughness of the blends in Single-Edge-Cracked-Plate configurations; all fracture behavior was followed extensively by SEM fractography.

Experiments demonstrated that the particles are attached to the matrix only through a differential thermal–contraction–pressure and particle separation preceded plastic response in all instances. As a consequence of the above ease in debonding, the yield strengths of the blends drop systematically with increasing particle concentration.

In slow tension all blends showed a well defined plastic stretching response following necking, but the stable post-necking stretch was severely limited by an overabundance of large particle clusters which acted as super-critical flaws to initiate premature termination of stretching. The present findings show that in these blends with their high plastic resistances, critical flaw sizes that trigger brittle response are in the range of 8–12 μm, well under the sizes of many of the particle clusters encountered in the blends.

In contrast with the attractively tough response of the rubber modified Nylon-6 blends of Muratoğlu et al. [Polymer 36 (1995) 921; Polymer 36 (1995) 4771] all present blends showed only disappointing brittle behavior under Izod impact conditions. This was traced to the development of substantial levels of triaxial tensile stresses arising from only partial separation of rigid particles from the matrix in the early phases of impact response.

Based on the new findings a number of general principles on toughenability with both compliant and rigid particle modification are presented and supported by simple micro mechanical models.

Keywords: Nylon-6/$CaCO_3$ blends; Toughenability of brittle polymers; Toughenability with stiff-particles

1. Introduction

Many, if not all polymers are intrinsically brittle and will behave as such at low temperatures and high strain rates, particularly when crack-like flaws are present. Toughening such polymers by altering the molecular microstructure [1] by modification with compliant or rigid heterogeneity particles (for an overview see Ref. [2]) by deformation-activated diluents [3] and a variety of other means is an active area of polymer research. There have been many models and rationalizations of mixed success and merit for such toughening that have been proposed (for a selection see e.g. Refs. [4,5]). A point of interest to us in these endeavors is the possibility of a proposition made by Wu [6] for the toughening of semi-crystalline polymers such as polyamides (nylon), HDPE, PP, etc. which states that when the interparticle matrix ligament dimension between equiaxed heterogeneities in the particle-modified-polymer is less than a critical value, specific for different polymers, a toughness jump should follow in impact experiments. The mechanistic basis of this proposition, which has created much controversy, has been clarified by Muratoğlu et al. [7] who have proposed that the incoherent particle-matrix interfaces stimulate a preferential form of crystallization over a definite distance around the particles with the lowest energy surfaces of crystalline lamellae representing also the crystallographic planes of lowest plastic resistance lying parallel to the interfaces. Such crystalline layers of large plastic anisotropy should result in local plastic

* Corresponding author. Tel.: +1-617-253-2217; fax: +1-617-258-8742.
E-mail address: argon@mit.edu (A.S. Argon).

0032-3861/01/$ - see front matter
PII: S0032-3861(01)00548-1

response at lower stress levels on planes parallel to the particle-matrix interfaces, and upon cavitation of particles, should result in overall lowered plastic resistance of the modified blend that makes it less susceptible to adventitious flaws which can trigger brittle behavior. Muratoglu et al. [7] have demonstrated the presence of such crystalline layers by a variety of quantitative techniques and found them to be of 0.15 μm thickness in Nylon-6. Thus, if the distance between particles is less than twice this distance the crystalline component of lowered anisotropic plastic resistance should percolate through the volume and initiate a tough response. The validity of these ideas was demonstrated by Muratoglu et al. [8,9] for rubber-modified Nylon-6, and by Bartczak et al. for both rubber and $CaCO_3$ particle-modified HDPE [10,11].

In preliminary experiments with $CaCO_3$-modified Nylon-6 blends poor results were obtained without properly ascertaining the cause of such failure. In the present study of toughenability of Nylon-6, modified with $CaCO_3$ particles the response of this system has been explored in depth, resulting in the identification of a number of general principles of toughening which have not only given definite explanations for the limited success in toughening of polyamides with rigid particles but have also provided guidelines on the toughenability of other polymers, of both semi-crystalline and glassy varieties. Among other things we present reasons why the critical ligament thickness criterion discussed above has been ineffective, particularly in relation with many other factors that negate its importance. These findings are discussed in what follows.

Table 1
Characteristics of calcium carbonate filler used in this study (these are all supplier data, elastic properties of CC are given in Section 4.1)

Filler code	Trade name	Supplier	Type and source	Density (g/cm^3)	Mean size of particles (by weight) (μm)	Surface area (m^2/g)	Geometrical standard deviation	Surface treatment
CC1	Hi-Pflex 100	Specialty Minerals Inc., USA	Ground limestone, Adams (MA)	2.7	3.50	3	2.98	Calcium stearate
CC2	Super-Pflex 200	Specialty Minerals Inc., USA	Precipitated from solution	2.7	0.70	7	1.61	Calcium stearate

2. Experimental procedure

2.1. Sample preparation

The polymer used in this study was Capron 8200^R Nylon-6 (polyamide 6) supplied by Honeywell) with a density of 1.14 g/cm^3. Two types of calcium carbonate (CC) particles were used as fillers. The characteristics of these are listed in Table 1. The particles were coated with calcium stearate, which in the past studies with HDPE resulted in better particle dispersion. The blends were prepared in two steps. First, polymer pellets were premixed with CC powder in desired proportions and then mixed in the molten state in a 30 mm Werner and Pfleiderer twin screw extruder. The extrusion-mixing process was performed at temperatures within the range of 190–200°C and a rotation speed of the screws of 200 rpm. Considerable effort was expended in achieving proper particle dispersion. The volume fractions were calculated with the densities of the Nylon-6 and CC and as given above and in Table 1. The resulting pellets were moulded in a 6 oz, 150 ton Van Dorn injection moulding machine into dog-bone-shaped tensile bars (ASTM D638-97 Type 1 specimen, 50 mm gauge length, 12.7 mm width, and 3.2 mm thickness) and flexural test bars (127 mm

length, 12.7 mm width and 3.2 mm thickness). The injection moulded flexural bars were then divided into two 63.5 mm long pieces, one close to the injection gate (hereafter called gate-end) and the other far from the gate (hereafter called far-end). This was done in the light of experience with HDPE/CC blends where important differences in behavior were found between these two parts [11]. Notches of root radius 0.254 mm were cut with a TMI Notching cutter according to the specifications of ASTM D256-97.

It is important to note that in this study two batches of blends were used. One series of blends was prepared in 1997, the other one in 2000, following nearly identical processing routines. The series from 1997 contained unmodified Nylon-6 and three blends of Nylon-6 with CC particles, each with a volume fraction of 0.28 CC. The three 1997 blends contained the same CC1 and CC2 filler particles. This series of materials was kept in storage in a dessicator. In addition to the long aging history of the 1997 blends they can be expected to have suffered changes in relative humidity. The 1997 batch of blends was processed in a 28 mm Werner and Pfleiderer twin screw extruder. In the present 2000 series of blends a wide range of volume fractions of filler particles was used. With the CC1 filler particles the volume fractions ranged over 0.1, 0.2, 0.4 while for the CC2 filler particles the volume fractions ranged over 0.05, 0.10, 0.15, 0.20, 0.25 and 0.28. Additionally unmodified Nylon-6 bars were also available for comparison. Table 2 lists the characteristics of all blends.

2.2. Mechanical probes

2.2.1. Tensile response

The tensile response of the dog-bone-shaped specimens of the blends were studied at −30, 20 and at 60°C, using an Instron 5582 tensile testing machine and an Instron 3119-007 heating chamber. The tests were performed according to ASTM D638-97 specifications at 50 mm/min crosshead speed, resulting in an initial strain rate of 1.6×10^{-2}/s. The samples were not conditioned prior to testing to remove or alter the water content. All specimens were handled in the exact same manner to make certain that they all contained the same concentration of water (for the effect of absorbed water on the mechanical response of Nylon-6 see Ref. [12]. They were kept in a dry dessicator until they were tested. The values of the mechanical response characteristics determined from these tests were obtained from the measurement of one specimen for each composition and test condition. Clearly, this curtailed procedure has resulted in no information on the variability in strains to fracture. For all the blends that were prepared in 1997, the values of the mechanical parameters are calculated as averages over five specimens for each composition. The 1997 blends were only tested at room temperature.

Table 2
Characteristics of blends used in this study

Material	Vol. %	Year made	Code
Unmodified Nylon-6	0	2000	1
Nylon-6/CC1	10	2000	2
Nylon-6/CC1	20	2000	3
Nylon-6/CC1	30	2000	4
Nylon-6/CC2	5	2000	5
Nylon-6/CC2	10	2000	6
Nylon-6/CC2	15	2000	7
Nylon-6/CC2	20	2000	8
Nylon-6/CC2	25	2000	9
Nylon-6/CC2	28	2000	10
Unmodified Nylon-6	0	1997	11
Nylon-6/CC1	28	1997	12
Nylon-6/CC2	28	1997	13

2.2.2. Impact response

The impact response was studied in notched Izod impact tests performed according to ASTM D256-97 standards. The pendulum speed at impact was 3.46 m/s. The tests were performed at room temperature. Kinetic energy and frictional loss corrections were made in accordance with ASTM D256-97 standards. While impact testing a distinction was made between gate-end and far-end specimens because of the possible influence of the conditions of the injection moulding process, as already stated above (see Ref. [11]).

For the blends prepared in 2000, the values of the Izod impact energies determined from these tests, were calculated as averages over measurements on two specimens for each composition. For the blends that were made in 1997, the values of the Izod impact energy were calculated as averages over six to nine specimens for each composition. Six tensile bars of each of the Nylon-6/CC2 blends were stretched in slow tension just up to the yield point. These pre-stretched tensile bars were then machined into flexural bars in order to study the impact response of pre-stretched and pre-cavitated Nylon-6/CC2 blends.

2.2.3. Single-edge cracked plate in uniform tension

To develop a rudimentary measure of the fracture resistance of the blends simple Single-Edge Cracked Plate (SECP) samples were used to determine a measure of fracture toughness at room temperature. Of each blend present in this study two SECP specimens were produced from the tensile bars. After performing the tensile test at room temperature, one of the broken ends of the tensile bar was taken and a SECP specimen was made from the cavitated part of it. The other specimen that was made from the same tensile bar was machined from one of the grip portions of the bar which had not experienced deformation, and thus, was not whitened. This SECP sample was used for comparison with the results of the pre-cavitated material. The dimensions of the SECP specimens were: length 38.2 mm, width 12.7 mm, and thickness 3.0 mm. The central cut was made with a 0.2 mm thick milling cutter to a depth of 4.2 mm, exactly halfway down the length of the specimen. The cut ‘crack’ was not sharpened further in

Table 3
The number of specimens of each blend that were tested at each different temperature

Code	$T = 20^{\circ}C$	$T = 60^{\circ}C$	$T = -30^{\circ}C$
1–9	1	1	1
11–13	5	0	0

any way. This needs to be noted in interpreting the results. The specimens were tested in an Instron 5582 tensile testing machine. The grips were placed 20 mm apart. The tests were performed at room temperature at a crosshead speed of 5 mm/min.

2.3. Scanning electron microscopy

Following the Izod and tension tests, the specimens were examined in a scanning electron microscope. A Philips XL30 FEG Environmental Scanning Electron Microscope (ESEM) was used for this purpose. The microscope was used in a high vacuum mode, at an operating pressure at 10^{-5} mbar. In order to prevent charging of the samples a thin (≈30 nm) coating of gold/palladium was deposited. This greatly improved the resolution of the images. The accelerating voltage used was 3.00 kV. A higher voltage would have improved the quality of the image but could not be used to avoid severe beam damage to the samples. The ESEM was used to study the morphology of fracture surfaces of the tensile specimens and Izod specimens, and to explore the deformation induced whitening behavior in the interior on axial cryo-fractured surfaces of both the tensile bars and the Izod bars. The protocol for such cryo-fracturing was described by Bartezak et al. [10,11]. The cryo-fracturing was performed by soaking the specimens in liquid nitrogen for at least 20 min, the specimens were then cleaved with a single edge razor blade while they were still near liquid nitrogen temperature. The revealed internal surfaces were then coated with gold/palladium (≈30 nm thickness), to prevent charging of the surface during microscopy.

3. Experimental results

3.1. Tension tests

As mentioned before, the tension tests were performed at three different temperatures: −30, 20 and 60°C. The number of specimens that were tested of each blend and at each different temperature are given in Table 3.

3.1.1. Tension tests at 20°C

Fig. 1 shows the engineering stress-extension behavior of the Nylon-6/CC blends. Fig. 1a shows the CC2 blends with volume fractions of particles ranging from 0 (plain Nylon-6) to 0.28. While Fig. 1b shows curves for the CC1 blends with volume fractions of particles ranging from 0 (plain Nylon-6) to 0.40. The tension tests were performed at 20°C and a cross head speed of 50 mm/min (initial strain rate 1.67×10^{-2} s^{-1}).

Table 4 presents the characteristic results calculated from these tests for each blend. It demonstrates that the Young's modulus of the blends increases with increasing volume fraction of CC filler. On the other hand there is a systematic decrease in yield stress and strain with increasing volume fraction of CC particles. In each case the yield stress was defined as the stress at peak load. In all cases this signifies the transition to fully developed plastic response. A comparison between the Young's moduli of blends with the same volume fractions of CC filler, but with a different filler type, show that the filler with large particles (CC1) causes a slightly larger increase of the modulus, compared to the unmodified Nylon-6, than the filler with the smaller particles (CC2). There is, however, no significant difference in the yield point between blends with different fillers but the same volume fraction.

Examination of the rising portions of all stress–strain curves, particularly those for the blends of the larger filler volume fractions showed a clear change in the slope well below the yield stress. This was taken as the stress where debonding of the filler particles occurs. Further visual observation of specimens of particle-modified Nylon-6

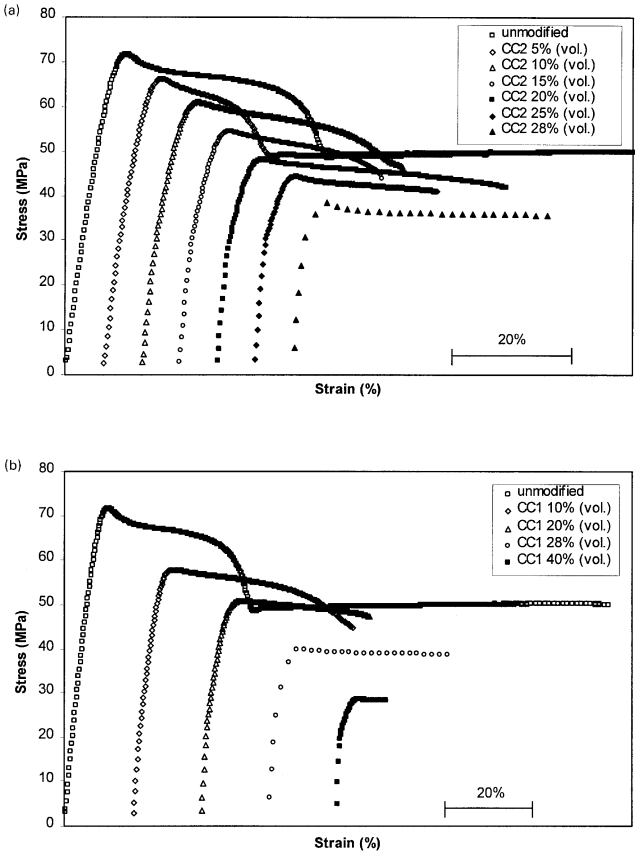

Fig. 1. Stress–strain curves of the series of Nylon-6 with (a) CC2 and (b) CC1 fillers. Tests were performed at 20°C. Each curve was shifted along the strain axis for clarity.

Table 4
Tensile properties of Nylon-6/CC blends at 20°C and an initial strain rate of 1.67×10^{-2} s^{-1}

Blend	Volumetric % filler	Young's modulus (MPa)[a]	Yield stress (MPa)	Yield strain (%)	Stress at break (MPa)	Elongation at break (%)
Nylon-6 (control)	0	1074.6	71.7	9.5	50.1	120.6
Nylon-6/CC1	10	1467.7	57.9	9.0	44.0	49.2
	20	1821.6	50.8	8.9	47.4	38.0
	28	1752.3	40.0	7.9	38.6	43.0
	40	2846.9	28.6	5.0	27.9	11.8
Nylon-6/CC2	5	1221.6	66.3	9.2	49.7	61.3
	10	1355.7	61.0	9.0	46.1	42.4
	15	1554.9	54.4	7.9	44.0	32.7
	20	1622.9	48.1	7.4	40.9	47.0
	25	1945.3	44.5	6.3	40.0	30.2
	28	1677.6	38.9	5.4	36.1	48.4

[a] As discerned from the initial slope of the stress–strain curves, see Section 4.1.

showed that prominent whitening of the blends occurs around the necking zone for all fillers and compositions studied. This confirms that debonding of the particles from the matrix had occurred before the yield point. The SEM results presented in Section 3.4 confirm this explanation.

The blends of the 2000 batch fractured mostly at the point where plastic flow began at the root of the flared out grip region. The unmodified Nylon-6 and the blends from the 1997 batch did not fracture at the previously mentioned point. In these the neck stretched more extensively and the specimen fractured later at a random point in the stretched zone.

SEM micrographs indicated that inclusions, consisting mostly of large clusters of CC particles and on some occasions large foreign particles (diameters between 50 and 200 μm), were responsible for the eventual fracture of the deforming blends and were found at all fracture origins. Thus, fracture in the necked zone occurred as soon as the border of the zone reached such an inclusion. In the case of the 2000 blends such inclusions were always present in the necked zone, causing the fracture. In the 1997 blends there were far fewer such inclusions present, permitting the neck to propagate a more substantial distance before reaching an outsize inclusion. Due to the chance encounter of the propagating neck with an inclusion, the ultimate elongations of the blends varied greatly. Such encounters of the neck with imperfections, while random, were not rare events, suggesting considerable improvements in performance could be possible if such clusters could be elimated as we discuss in Section 4.4 below. In many blends such undesirable premature fractures were too common to prevent reaching a stable stretching response. Therefore, to make a comparison between the levels of flow stress of the different blends, the levels of the stress at break was taken. The flow stress (stress at break) generally decreases as the filler content increases but not as strongly as the yield stress decreases (see Fig. 1). The elongation at break is in general decreasing with increasing CC volume fraction due to increasing probabilities of encounter with outsized inclusions, as discussed above. Similar observations were also made by Bartczak et al. in HDPE with CC fillers [11].

Fig. 2 shows the difference between the unmodified Nylon-6 behavior from the 1997 batch (aged) and the 2000 batch (not aged). A comparison between these tensile responses shows that the aged Nylon-6 has a slightly lower Young's modulus, a lower yield stress and a lower flow stress. This reduction could well have been caused by some water pick up over the intervening 3 years. Both curves show prominent yield phenomena associated with a drop in the stress level after yielding followed by a region of small decrease in stress and then another large drop in the stress level upon development of a neck. Visual observations showed whitening at the point of the yield drop. At the second drop, related to necking, the already whitened material stretched out and became transparent in the unmodified nylon samples. In the flow region the whitened zone propagates outward to produce a nearly transparent material. Thus, the unmodified material first whitens at the shoulder and later becomes more transparent in the stretched zone. Peterlin [13] has described this phenomenon for

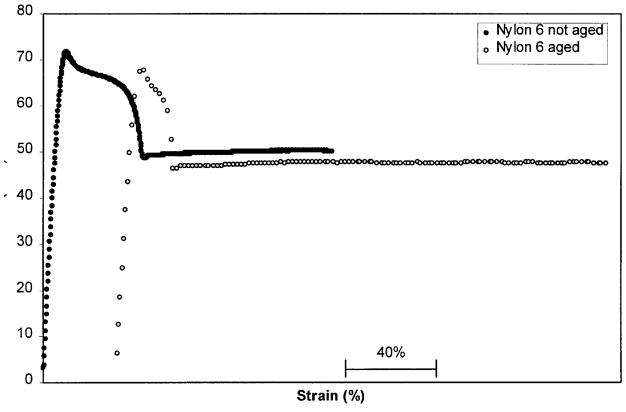

Fig. 2. A comparison between the stress–strain behavior of the unmodified Nylon-6 from the batch form 1997 and 2000. The curves are shifted for clarity.

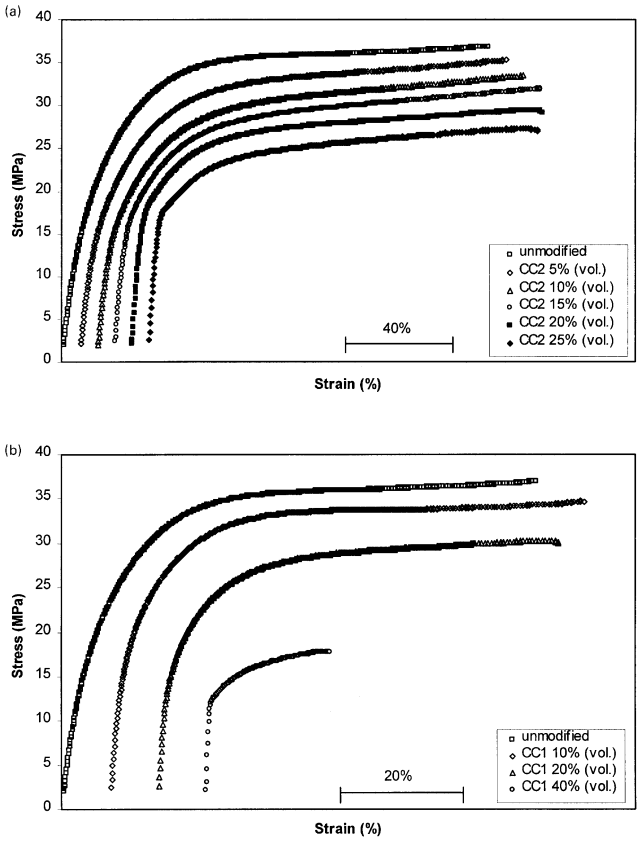

Fig. 3. Stress–strain curves of the series of Nylon-6 with (a) CC2 and (b) CC1 fillers. Tests were performed at 60°C. For clarity each curve was shifted along the strain axis. The unmodified Nylon-6 and the blend with volume fraction of 0.10 of CC1 did not break. The blends with volume fractions of 0.05, 0.10 and 0.15 of CC2 also did not break.

polyethylene and polypropylene and called the behavior 'micronecking'. From Fig. 2 it is clear that the aged Nylon-6 does not cavitate as readily as the un-aged Nylon-6 of the 2000 blend.

3.1.2. Tension tests at 60°C

Fig. 3a and b show the stress–strain behavior of the Nylon-6/CC blends with volume fractions between 0 (plain Nylon-6) and 0.25 for CC2 and volume fractions between 0 (plain Nylon-6) and 0.40 for CC1. These tension tests were performed at 60°C and a crosshead speed of 50 mm/min. Table 5 presents the results calculated from these tests for each blend. It demonstrates that the Young's modulus of the blends increases with increasing volume fraction of CC filler. Compared to the Young's moduli at room temperature, for each of the blends at 60°C the Young's moduli are considerably smaller, usually by a factor of 3. This is consistent with a glass transition occurring in the amorphous component around 35–40°C [14]. A comparison between the Young's moduli of blends with the same volume fraction of CC filler, but with different filler type, show that the filler of larger particles (CC1) causes a somewhat larger increase of the modulus, compared to the unmodified Nylon-6 at 60°C, than the filler with the smaller particles (CC2). There is a very protracted transition to fully developed plastic flow in all cases, reaching eventually a slow hardening behavior. There is no yield phenomenon and localization of flow by necking is absent.

The hardening rate has increased compared to the unmodified Nylon-6, except for the Nylon-6/CC1 blend with 0.05 filler. There is no correlation between hardening rate and volume fraction of CC filler. Elongation at break increased considerably compared to the elongation at break at room temperature. Visual observations showed that after the transition to plastic flow whitening occurred in the whole gauge region. The unmodified Nylon-6 did not whiten but became progressively more transparent. This is a direct consequence of the absence of necking and the lack of formation of triaxial stresses in the shoulder region.

3.1.3. Tension tests at −30°C

Fig. 4a and b show the stress–strain behavior of the Nylon-6/CC blends performed at −30°C at a cross head speed of 50 mm/min. The response of the blends with CC2 particles with volume fractions ranging between 0 and 0.25 are shown in Fig. 4a, while those with CC1 particles with volume fractions between 0 and 0.40 are given in Fig. 4b. Table 6 presents the basic results calculated

Table 5
Tensile properties of Nylon-6/CC blends at 60°C and an initial strain rate of 1.67×10^{-2} s^{-1}

Blend	volumetric % filler	Young's modulus (MPa)	Yield stress (MPa)	Yield strain (%)	Hardening rate (kPa)	Stress at break (MPa)	Elongation[a] at break (%)
Nylon-6 (control)	0	265.5	9.3	3.7	15.4	–	>150
Nylon-6/CC1	10	458.7	11.0	2.6	12.0	–	>150
	20	546.2	11.1	2.2	21.7	30.2	124.2
	40	775.4	11.7	1.7	74.2	17.8	38.7
Nylon-6/CC2	5	311.0	8.9	3.1	26.4	–	>150
	10	331.5	9.9	3.2	31.2	–	>150
	15	384.7	11.5	3.2	30.2	–	>150
	20	463.3	12.3	2.9	22.1	29.4	141.7
	25	547.9	11.8	2.4	27.9	27.2	133.9

[a] Some samples did not break as a result of physical limitations of the heating chamber, they reached the maximum extension of 75 mm.

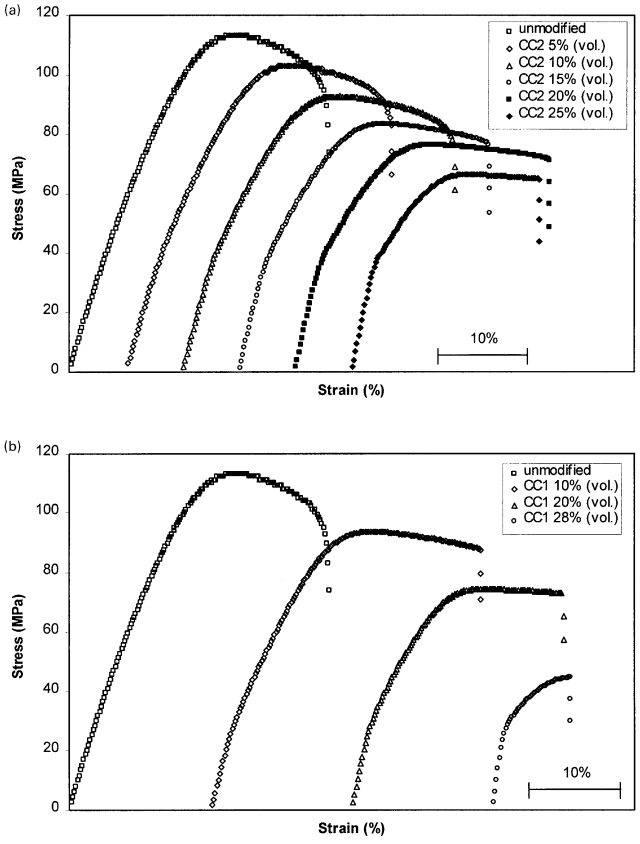

Fig. 4. Stress–strain curves of the series of Nylon-6 with (a) CC2 and (b) CC1 fillers. Tests performed at −30°C. For clarity each curve was shifted along the strain axis.

from these tests for each blend. It demonstrates again that the Young's modulus of the blends increases with increasing volume fraction of CC filler. Compared to the Young's moduli at 20°C, for each blend the Young's moduli are slightly smaller which is against expectations and must result from the changed stiffness of the pull rods in the load train, as discussed in Section 4.1. A comparison between the Young's moduli of blends with the same volume fraction of CC filler, but of different filler type, show that the filler with larger particles (CC1) results again in a somewhat larger increase of the modulus, compared to the unmodified Nylon-6 at −30°C, than in the case with the filler with the smaller particles (CC2). This too is attributed to difficulties in making precise assessments from the initial slope of the stress strain curves.

The tensile strength and tensile strain at fracture decrease with increasing volume fraction of CC filler. The tensile strength was closely similar for the blends with the same volume fraction CC1 or CC2 filler particles. Visual observations showed that the unmodified Nylon-6 neither whitened nor became transparent. The particle-modified blends did whiten somewhat. In these latter blends necking did not progress because of rapid subsequent fracture. In the unmodified Nylon-6 and the CC2 blends with 0.05 and 0.10 volume fraction of particles, necking occurred, but was not followed by significant post-necking stretching, accounting for the absence of stretch-induced transparency in the unmodified nylon. There were no prominent yield phenomena as in the tests at 20°C.

3.2. Izod impact response

Table 7 lists the number of samples tested in each category. The materials with codes 1–10 were those prepared in 2000, while those with codes 11–13 had been prepared in 1997. Fig. 5 shows the notched Izod impact energies, I_s, measured at room temperature of the samples of the batch prepared in 2000. The measured I_s energies of plain Nylon-6 and various Nylon-6/CC2 blends are shown in Fig. 5a and those of the various Nylon-6/CC1 blends are shown in Fig. 5b. Data for specimens cut from the gate-end and the far-end of the flexural bars are shown separately for each blend. These data shown are averages of two measurements; the error bars show the range. For all compositions tested there was a distinct difference in toughness between the gate-end and the far-end specimens. This difference is attributed to differences in the flow pattern in both parts of the mould during the injection-moulding process. Similar differences observed in the HDPE blends could not be definitively traced to a specific cause [11].

Fig. 5 shows that all of the Nylon-6/CC2 blends are tougher than plain Nylon-6, whereas all of the Nylon-6/CC1 blends are less tough than plain Nylon-6. There is no

Table 6
Tensile properties of Nylon 6/CC blends at −30°C and an initial strain rate of 1.67×10^{-2} s^{-1}

Blend	Volumetric % filler	Young's modulus (MPa)	Tensile strength (MPa)	Strain at Tensile strength (%)	Stress at break (MPa)	Elongation at break (%)
Nylon-6 (control)	0	1069.5	113.0	17.6	89.7	28.1
Nylon-6/CC1	10	1280.8	93.5	16.8	87.1	29.7
	20	1576.7	74.5	14.3	72.6	23.2
	40	2252.2	44.6	8.3	44.5	9.2
Nylon-6/CC2	5	1139.0	103.1	17.6	85.2	29.0
	10	1256.8	92.9	16.8	77.5	29.7
	15	1364.4	83.5	15.9	76.5	27.5
	20	1474.6	76.6	14.3	70.6	27.9
	25	1589.3	66.7	12.6	64.6	20.8

Table 7
Number of samples tested in Izod experiments in each category

Code	1997	2000
1–9	–	2
11–13	2–4	6–9
1 + 5–10 prestretched	–	6

significant dependence of I_s on the volume fraction of the filler in the toughened Nylon-6/CC2 blends. Fig. 5a also shows the Izod impact energies of the pre-stretched are pre-cavitated samples of the Nylon-6/CC2 blends as the white columns. The values are averages of six measurements and the error bars are the standard deviations. Clearly, these values are lower than those of the other corresponding impact energies for each blend that is present, indicating that pre-stretching to yield had compromised some of the potential for tough response.

In all the tests the specimens broke completely. In the plain Nylon-6 and the Nylon-6/CC2 blends with volume fractions of 0.05 and 0.10 the crack bifurcated immediately at the notch in both the gate-end and far-end samples. This was not observed in any other blend. So, to compare the results of these blends with the others it should be noted that the impact energy would have been considerably lower if the crack had not bifurcated. None of the pre-stretched samples bifurcated. This accounts for a sufficient part of the difference between the impact energies of the pre-stretched bars and those of the gate-end and far-end samples. The reason why this bifurcation appears remains uncertain. Additional measurements on samples from the same batch but notched in a different way, also showed bifurcation of the crack. The measured impact values of these tests showing bifurcation are shown in Fig. 5a with dashed lines, labeled (wb), 'with bifurcation'.

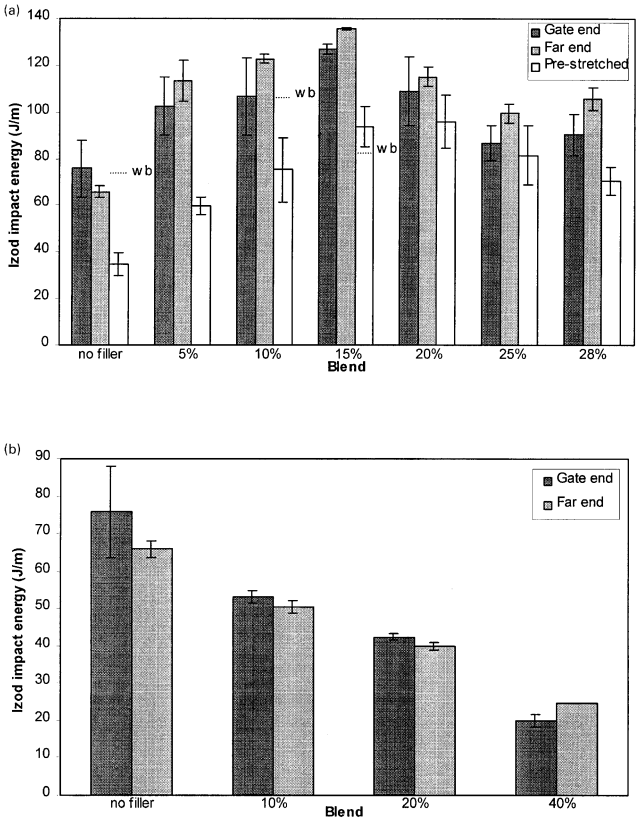

Fig. 5. Notched Izod impact energies measured at 20°C for (a) unmodified Nylon-6 and Nylon-6/CC2 blends; (b) pure Nylon-6 (no filler) and Nylon-6/CC1 blends. Izod impact energies for gate end and for far end specimens are shown separately.

The fracture surfaces of the plain Nylon-6 and the Nylon-6/CC1 specimens did not show any whitening. On the fracture surfaces of the Nylon-6/CC2-blend specimens in a region from the end of the notch up to 2 mm away from it, some whitening was visible. SEM observations showed very brittle fracture surfaces for all the specimens, but gave clear evidence of debonding of the CC2 particles, as we discuss in Section 3.4.2.

Fig. 6 shows the Izod impact energies of the materials from the 1997 batch. These blends all contained 0.28 volume fraction of CC filler particles. One pair of gate-end and far-end Izod impact energies was measured in 1997 and the other pair of gate-end and far-end Izod impact energies was measured in 2000. Both series of measurements were done at 20°C. The only difference between both series of measurements is the time at which the tests were performed and thus the length of time that they were stored. The data shown are averages of two to eight measurements. The error bars represent the standard deviations. The increased contact with air had the effect of somewhat toughening of all of the 1997 blends. The relative increase in toughness in the Nylon-6/CC1 blend is considerably smaller than in the other blends. For the other blends the relative increase in I_s was about 200%.

3.3. Single-edge cracked plate in uniform tension

To obtain a better measure of the crack growth resistance

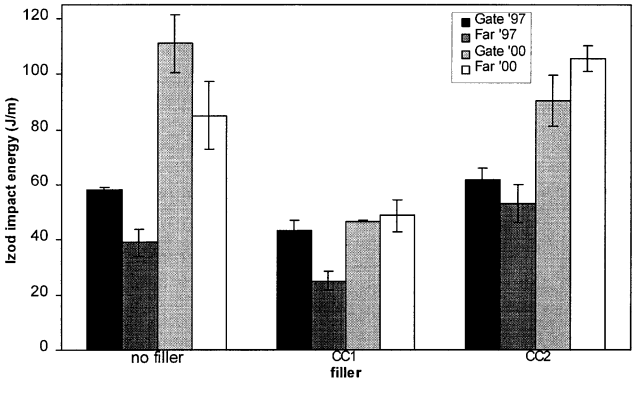

Fig. 6. Notched Izod impact energies measured at room temperature for the blends prepared in 1997. These blends all contain 0.28 volume fraction of CC filler. One pair of gate end and far end Izod impact energies was measured in 1997. The other pair of Izod impact energies was measured in 2000.

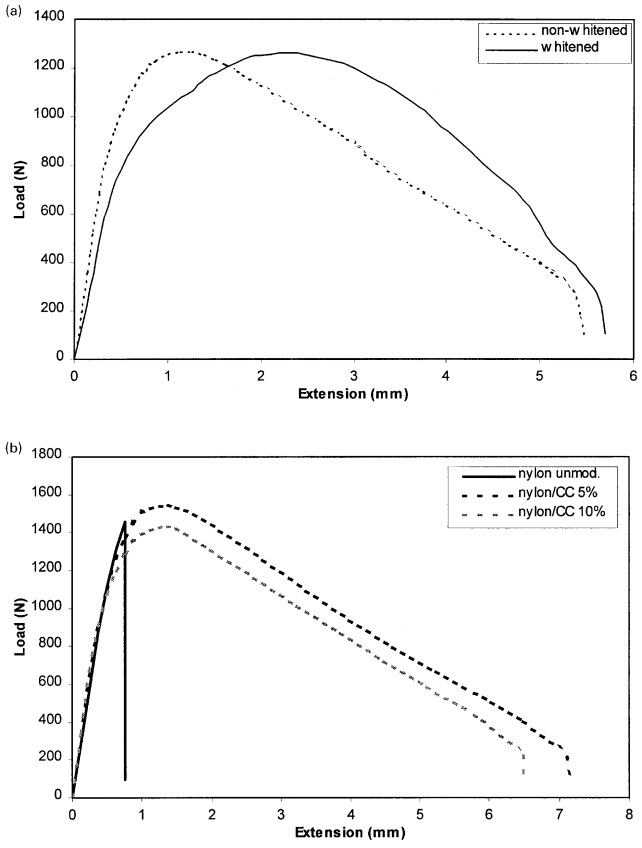

Fig. 7. (a) Load-extension curves of the whitened and non-whitened SECP specimen from the Nylon-6/CC blend with 0.15 of CC2. The tests were performed at 20°C at a crosshead speed of 5 mm/min. (b) Load-extension curves of the non-whitened SECP specimens from the unmodified Nylon-6 and the Nylon-6/CC2 blend with 0.05 and 0.10 filler respectively. The tests were performed at 20°C at a crosshead speed of 5 mm/min.

in the cavitated and porous blends, SECP samples were tested to obtain a measure of the fracture work through the determination of the J integral toughness. This better characterizes the propagating crack environment for the inception of the fracture process of materials undergoing large strain plasticity. Fig. 7a shows the characteristic tensile separation behavior of non-whitened and whitened blends modified with CC2 particles at a volume fraction of 0.15. Fig. 7b shows the load extension curves of the unmodified Nylon-6 and the non-whitened blends with CC2 particles at volume fractions of 0.05 and 0.10. The brittle response of the unmodified by Nylon-6 compared to the response of the Nylon-6/CC2 blends is evident. The specimens that were used were machined from fractured pieces of the tensile bars of the Nylon-6/CC2 blends with volume fractions ranging between 0 and 0.25 and Nylon-6/CC1 blends with volume fractions ranging between 0 and 0.40. The declining portion of the tearing load is a result of the decreasing width of the untorn specimen, and signifies a tough response. The J integral toughness, for a SECP type specimen, is given by the following expression: [15],

$$J = \alpha\epsilon_0 Y_0(1-\psi)ch_1(a/b,n)(P/P_0)^{n+1} \tag{1a}$$

where α is a material constant; ϵ_0 is the strain at yield; Y_0 the yield stress; ψ is the volume fraction of the CC particles; a is the crack length; b the width of the specimen; $c = b - a$; n is the strain hardening exponent; h_1 is a tabulated function of a/b and n, and is obtained from numerical solutions of the crack tip field; t_s is the specimen thickness; P is the load per unit thickness t_s; and P_0 the plane stress limit-load is given by:

$$P_0 = 1.072\eta c Y_0(1-\psi) \tag{1b}$$

$$\eta = [1 + (a/c)]^{1/2} - \frac{a}{c} \tag{1c}$$

In the evaluation of J the following values were used for the specimen of the type in Fig. 1: $a = 4.2$ mm; $b = 12.7$ mm; $c = 8.5$ mm; $t_s = 3.0$ mm; $\eta = 0.62$. For the material parameters the following quantities were used, determined by Lin and Argon [14]: $\alpha\epsilon_0 = 3.95 \times 10^{-3}$; $Y_0 = 71.7$ MPa; $n = 2.70$. The numerical parameter $h_1 = 2.38$ was determined by interpolation from tabulated information of the SECP specimen for the parameters given above, for a plane stress problem. As Fig. 8 of the fractured surface of the non-whitened specimen of the Nylon-6/CC2 blend with 0.1 volume fraction filler shows clearly, quite considerable lateral thinning occurred in all of the specimens during stretching prior to crack growth indicating that the separation was indeed behaving in a plane stress mode.

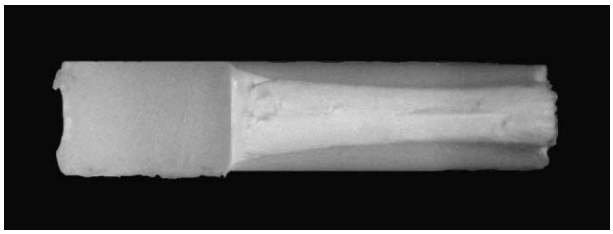

Fig. 8. Reduction of cross-sectional area in the SECP specimen of the Nylon-6/CC2 blend with 0.1 filler.

As a specific example consider the whitened Nylon-6/CC2 blend with a volume fraction of 0.15 of particles in which the peak load per unit thickness was 409 kN/m and $P_0 = 342$ kN/m was calculated for the given data, giving a J integral toughness of $J = 9.39$ kJ/m^2. Fig. 9a shows the J integral values for whitened and non-whitened Nylon-6/CC2 blends as a function of the volume fraction of CC2 filler. Fig. 9b shows the same information for blends with CC1 filler. Table 8 gives the values of the calculated J integrals of all the non-whitened and whitened samples. It shows that for each blend the J integral value of the non-whitened material is higher than for the whitened material indicating a certain amount of stretch work had already been 'expanded' in cavitating the material. There is a decrease in the J integral values of the blends with increasing volume fraction the CC1 and CC2 filler, as can be expected and, as

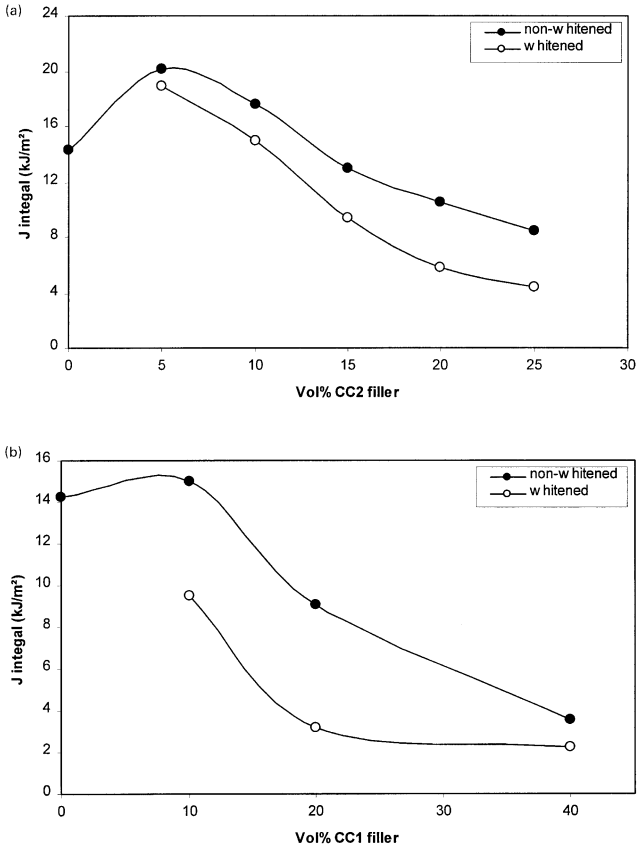

Fig. 9. *J* integral value of different Nylon-6/CC blends plotted against the volume fraction of CC filler: (a) for CC2 filler, and (b) for CC1 filler. The tests were performed at 20°C and a cross head speed of 5 mm/min.

explained in Section 4.3. The relatively low value of the *J* integral of the unmodified Nylon-6 becomes clear from Fig. 7b. The brittle response causes a fracture at low extension and load-level, resulting in a relatively low *J* integral value.

3.4. Fractography

3.4.1. Tension samples

Following the tension tests, the fractured specimens were examined by scanning electron microscopy. Fig. 10 shows

Table 8
J integral values for various blends for the non-whitened region and the whitened region

Blend	Volumetric % filler	*J* integral (kJ/m^2) non-whitened region	*J* integral (kJ/m^2) whitened region
Nylon-6 (control)	0	14.3	
Nylon-6/CC1	10	15.0	9.5
	20	9.1	3.2
	40	3.6	2.2
Nylon-6/CC2	5	20.1	19.0
	10	17.6	14.9
	15	13.0	9.4
	20	10.6	5.9
	25	8.5	4.4

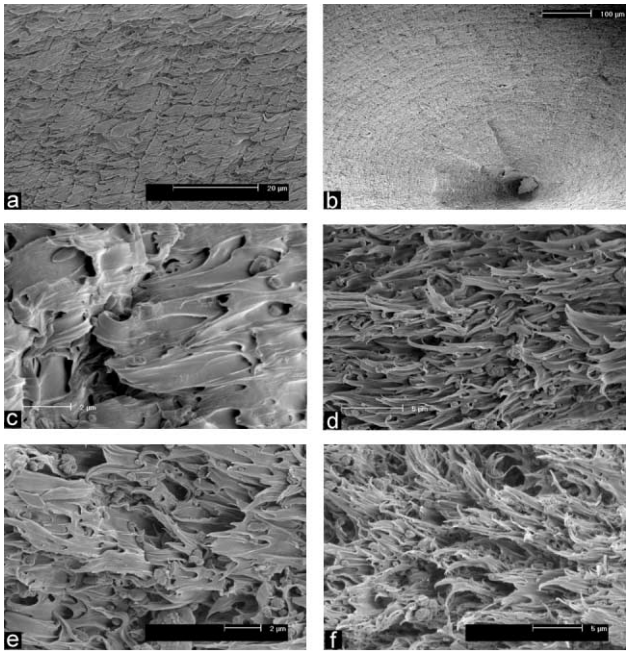

Fig. 10. SEM fractographs of the fracture surfaces of tensile bars of Nylon-6/CC2 blends: (a) no filler, (b) 0.05, (c) 0.05 at higher magnification, (d) 0.1, (e) 0.15, (f) 0.2 filler. In the higher magnification fractographs the direction of crack propagation is from right to left.

the SEM fractographs of tensile bars of unmodified Nylon-6 and of Nylon-6/CC2 blends with volume fractions of 0.05, 0.1, 0.15 and 0.2 CC2 filler. Fig. 10a and b show fracture surfaces at low magnification for unmodified Nylon-6 and the Nylon-6/CC2 blend with 0.05 vol. fraction CC2 filler respectively as representative cases. Regular striations appear on the fracture surfaces perpendicular to the direction of propagation of the crack. These striation patterns were only visible in the unmodified Nylon-6 and Nylon-6/CC blends with volume fractions of 0.05 and 0.10 filler. Bartczak et al. have reported the same patterns in HDPE/rubber blends [10] and in HDPE/CC blends [12], Muratoğlu et al. have reported these for rubber modified Nylon-66 [16]. Fig. 10c is an enlarged region of Fig. 10b. It shows the extensive plastic stretch of the Nylon-6 ligaments between the debonded CC2 particles. Fig. 10d–f show the same stretched ligaments in Nylon-6/CC2 blends with volume fractions of 0.10, 0.15 and 0.20 of CC2 filler particles. The direction of crack propagation is from right to left. The high magnification fractographs show nearly complete separation of the debonded particles and at these levels of stretch of ligaments are apparently offering no important resistance. The very extensive stretches of the ligaments shown in Fig. 10c–f, readily in the range of extension ratios of 5.0 or larger, give the impression of possibly substantial adiabatic heating effects in the later stages of separation. The V-shaped deformation markings on the Nylon-6 fracture surface as shown in Fig. 10a are seen in areas close to the fracture origins. In the unmodified samples these features are likely to be a consequence of the earlier

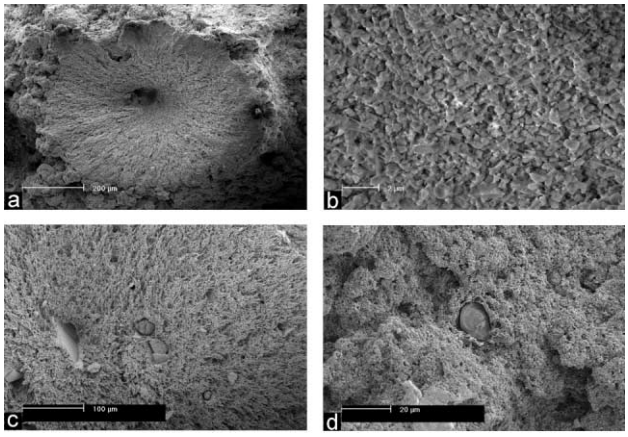

Fig. 11. SEM fractographs of the fracture surfaces of tensile bars of Nylon-6/CC2 blends. (a) and (b) of the blend with 0.1 filler and (c) and (d) of the blend with 0.2 filler. (a) shows a fracture origin surrounded by an elliptical zone of tough ligament stretching response. (b) shows the surface of a large inclusion at high magnification, demonstrating that the inclusion is a very large particle cluster. (c) and (d) show that a large concentration of inclusions is present at the fracture surfaces of the Nylon-6/CC2 blend with 0.2 of CC2 filler. (c) is from a region closer to the fracture origin than the area shown in (d) which is outside the elliptical ligament stretch zone.

cavitation at the shoulders and the so-called 'micronecking' response discussed above. Due to adiabatic heating the deformed ligaments lay on their side as if being 'brushed' in the direction of crack growth. All the Nylon-6/CC2 blends give much evidence of initiation of independent fracture nuclei by large clusters of particles and other inclusions. Large particles or clusters of CC2 particles with diameters between 40 and 200 μm were frequently found on the fracture surfaces with the V-shaped deformation markings and ruptured tips of ligaments pointing away from these origins. Most inclusion-initiated origins were of 'crater' shape, as in Fig. 10b. Fig. 11a shows a typical crater shaped fracture origin in a CC2 blend with 0.10 particle concentration. Several of these 'craters' were found on each fracture surface of the Nylon-6/CC2 blends. Higher magnification inspection of most inclusions, initiating such fracture, showed that they consisted of very large clusters of the CC2 filler particles. Fig. 11b shows the surface of a typical large inclusion cluster of particles, with individual particles being clearly resolvable. Fig. 11c demonstrates that there is an abundance of such particle clusters revealed on a typical fracture surface. The area of Fig. 11c is still in the elliptical crater region close to where the fracture started. Fig. 11d shows how the fracture surface looks outside the crater region, having the appearance of a sponge-like brittle form. These were characteristic features of all Nylon-6/CC blends. Even in these brittle sponge-like areas the blend has cavitated and the material has become porous. Fig. 11c and d were taken from a blend with CC2 particles of 0.15 concentration.

The fractographs of Fig. 12a and b were taken from a Nylon-6/CC1 blend with 0.2 particle concentration. In general the fracture surfaces of the blends with CC1 filler

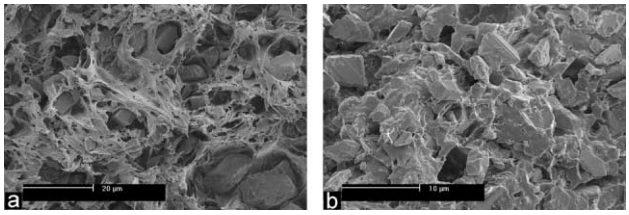

Fig. 12. SEM micrographs of the fracture surface of the tensile bar of the Nylon-6/CC1 blend with 0.1 of filler: (a) a 'ductile' region and (b) a brittle region.

particles have a distinctly brittle appearance. In those with 0.10 and 0.20 particle concentration in some small regions on the fracture surfaces debonding of the CC1 particles and plastic deformation of the Nylon-6 was observable. In the 0.40 vol. fraction blend no debonding or plastic deformation was apparent. However, the breaks in the slopes of the stress strain curves in the elastic region indicate that debonding of particles had always preceded yielding. Fig. 12a shows a region on the fracture surface with considerable plastic stretching of the Nylon-6 ligaments. Fig. 12b shows a brittle part of the fracture surface. The latter figure is more representative of the fracture surfaces of these blends. On all of the Nylon-6/CC1 blends there were no regions showing unambiguous crater-like fracture origins as in the CC2 blends. This is attributed to the quite large average size and wide size distribution of the CC1 particles with most of them acting as independent fracture origins already. In contrast to the CC2 filler particles, the CC1 filler particles have a very rough appearance with sharp edges, no doubt, resulting from their 'as ground' origins (see Table 1). Fig. 12a and b illustrate these sharp edges of the CC1 particles. While the supplier data gave 3.5 μm as the average particle diameter, many particles observed had far larger sizes. A significant fraction of particles had diameters above 10 μm, verifying the above observation that they constituted independent fracture origins as we discuss further in Section 4.6.

The broken tensile specimens were also cryo-fractured as described earlier in order to study the morphology of the evolving deformation process in the bulk of the specimens. Fig. 13 shows some cryo-fractographs taken from the tensile specimen of a Nylon-6/CC2 blend with 0.10 CC2 filler concentration. The diagram associated with Fig. 13 shows the locations from which the observations were made. In all the micrographs the fracture surface is above the figure. The distances from the crack-plane for Fig. 13a–d are respectively: 0.1, 0.8, 1.5 and 2.2 mm. All micrographs illustrate clearly that Nylon-6 cavitates and stretches after extensive debonding of the CC2 particles. The degree of stretching of the ligaments decreases with increasing distance away from the crack plane. This distribution of stretching in bulk of Nylon-6 was nearly the same for all Nylon-6/CC2 blends.

In all the Nylon-6/CC2 blends clusters of CC2 particles of various sizes have been observed, as already stated above.

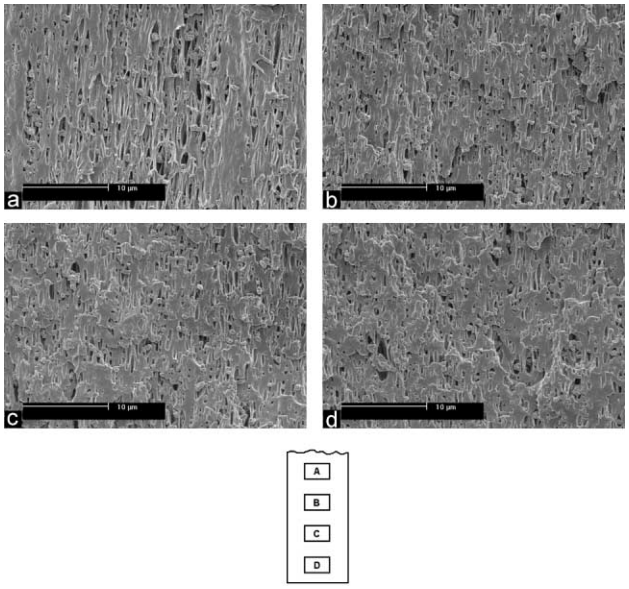

Fig. 13. SEM micrographs of the bulk of the tensile bar of the Nylon-6/CC2 blend with 0.1 of CC2 filler. The distances away from the crack plane of the region of the micrographs are depicted in the attached sketch and are at distances of: 0.1, 0.8, 1.5 and 2.2 mm, respectively below the fracture plane.

Especially in the blends with volume fractions of 0.20 and 0.25 CC2 particles, where particle touching probabilities are already high, even when randomly dispersed, high concentrations of such clusters were found, indicating that they are a feature of the material preparation process. Fig. 14 shows examples of these clusters found in the blend with 0.25 CC2 particle concentration, in an axial cryo-fracture plane taken 0.9 mm below the fracture surface.

In the Nylon-6/CC1 blends the density of separated particles and developing cavities in the bulk of the broken tensile bars is much lower compared to the Nylon-6/CC2 blends. The cavities that are present are bigger, and ill shaped, which is not only due to the larger average particle size but also due to their more angular and rough shape. This is illustrated in Fig. 15. It should be noted that the stretching of the nylon ligaments does not increase significantly with decreasing distance from the crack plane.

3.4.2. Izod impact samples

Following the Izod impact tests, the gate-end specimens were examined by scanning electron microscopy. Fig. 16a–d

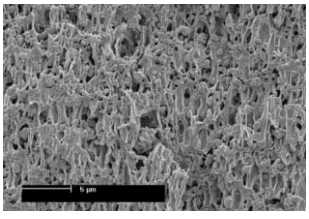

Fig. 14. SEM micrograph taken 0.9 mm below the fracture plane of the blend with 0.25 volume fraction of CC2 filler.

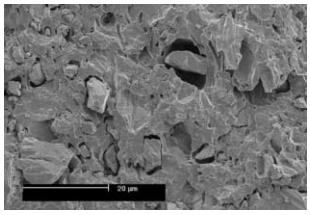

Fig. 15. SEM micrograph taken 3.0 mm below the fracture plane of the blend with 0.20 of CC1 filler.

show SEM fractographs of the fracture surface of unmodified Nylon-6. The micrographs were taken at four different places at the fracture surface depicted on the attached diagram, at increasing distances of 0.3, 2.5, 5.0 and 7.5 mm away from the root of the notch. The fracture surface had a uniformly very brittle appearance. Long grooves, parallel to the direction of crack growth, usually referred to as 'river markings' were present. Fig. 17a–d show fractographs taken from the fracture surface of the broken Izod sample of the Nylon-6/CC2 blend with 0.15 CC2 filler particle concentration at the same distances from the root of the notch as in Fig. 16. In both sets of figures, the crack propagated from left to right. Fracture surfaces of the other Nylon-6/CC2 blends also had a similar appearance of complete brittleness. A remarkable difference of the particle modified blends from the fracture surface of the unmodified nylon is that the surfaces look 'spongy' and there are larger height differences in a 'terraced' type of fracture surface. This type of terraced fracture behavior where the fracture surface is made up of a collection of smaller fracture planes at different heights due to a large number of independent crack initiations ahead of the main

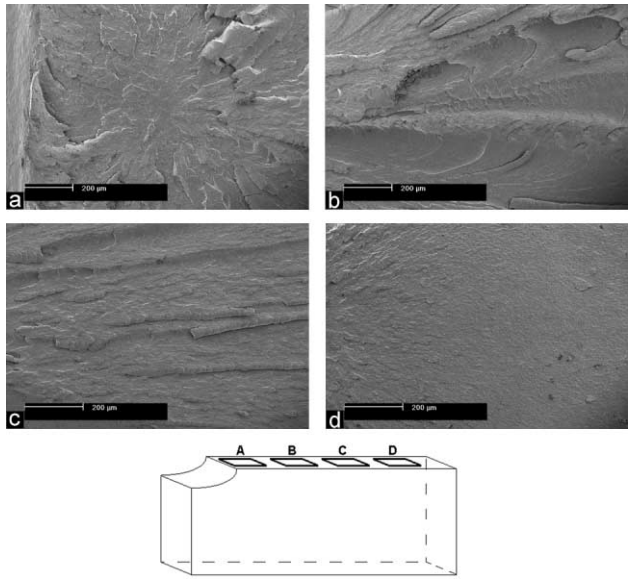

Fig. 16. SEM fractographs of the broken Izod sample of unmodified Nylon-6. The fractographs were taken at increasing distances away from the root of the notch at: 0.3, 2.5, 5.0 and 7.5 mm from the root of the notch as depicted in the attached sketch. The crack propagated from left to right.

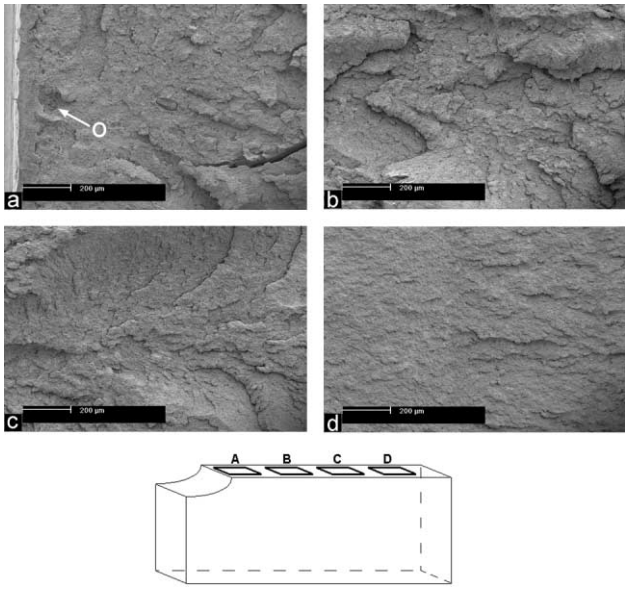

Fig. 17. SEM fractographs of the broken Izod sample of the Nylon-6/CC2 blend with 0.15 of CC2 filler. The fractographs were taken at increasing distances from the root of the notch, taken at distances of respectively: 0.3, 2.5, 5.0 and 7.5 mm from the root of the notch, as depicted in the attached sketch. The crack propagated from left to right.

crack, arising from the internal heterogeneities is referred to as 'crack deflection toughening' and accounts for a modest increase in toughness relative to a purely planar form of fracture [35]. The surfaces of the Nylon-6/CC1 blends also looked very similarly brittle and spongy.

In Fig. 17a an inclusion is visible in the crack origin marked with 'o'. Fig. 18a and b show micrographs of crack origins of the Izod samples of the Nylon-6/CC2 blends with 0.10 and 0.25 particle concentrations respectively. In these fracture origins large inclusions having diameters of 50–100 μm are also visible in the central region. For all the Izod samples Figs. 16–18 show that the fracture started about 250 μm ahead of the root of the notches, which had radii of the same magnitude, i.e. 254 μm. This suggests some local plastic flow and blunting of the crack tip had occurred prior to fracture initiation. Around the inclusion in the fracture origin of the Izod sample of the blend with 0.25 volume fraction of particles some evidence of plastic deformation of the Nylon-6 is observable, supporting the above conclusion.

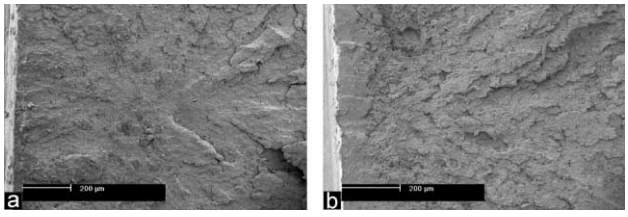

Fig. 18. SEM fractograph showing fracture origins of the Izod impact samples of the Nylon-6/CC2 blend with (a) 0.1 of CC2 filler and (b) 0.25 of CC2 filler. The root of the notch is visible in the left side of the pictures.

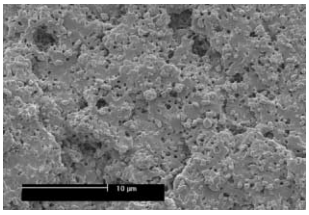

Fig. 19. SEM fractograph of the cavitation on the Izod impact specimen fracture surface of the Nylon-6/CC2 blend with 0.15 of CC2 filler.

At higher magnification a high density of shallow cavities was observable on the fracture surfaces of the Izod samples of the Nylon-6/CC2 blends. Fig. 19 shows an example of the source of the spongy appearance at lower magnifications in a blend with 0.15 filler concentration. This furnishes evidence that even in the impact samples debonding preceeds fracture. On this micrograph several moderate size clusters of CC2 filler are observable, especially on the surface of the blend with 0.25 filler fraction.

The broken far-end Izod impact specimens were also cryo-fractured in order to study the morphology of the bulk deformation of the specimens. In either the unmodified Nylon-6 or the Nylon-6/CC1 blends no significant evidence of plastic deformation was observed in the bulk. In isolated cases in some of the Nylon-6/CC2 samples, however, small regions were found where plastic deformation had taken place. This was usually in the form of a layer of 50 μm thickness parallel to the fracture surface at a depth of about 50 μm. Fig. 20 shows an example of such a layer, on a cryo-fracture plane of a Nylon-6/CC2 blend with 0.10 filler concentration. Fig. 20a and b show such a layer at two levels of magnification.

4. Discussion

4.1. Elastic properties of blends

The principal purpose of using inorganic filler particles in toughening is to derive a beneficial enhancement of elastic properties in the blends in addition to improvements in toughness. This enhancement for the present blends, tested at 20°C and −30°C was reported in Tables 4 and 6. Considering first the Young's modulus of unmodified nylon we note little change in the measured quantities between 20°C

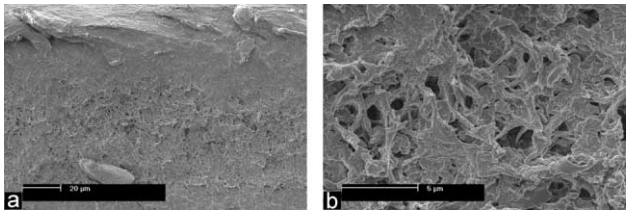

Fig. 20. SEM cryo-fractograph in the Izod-1 plane of the Izod impact specimen of the Nylon-6/CC2 blend with 0.10 of CC2 filler, just below the surface: (a) at low magnification; and (b) at high magnification.

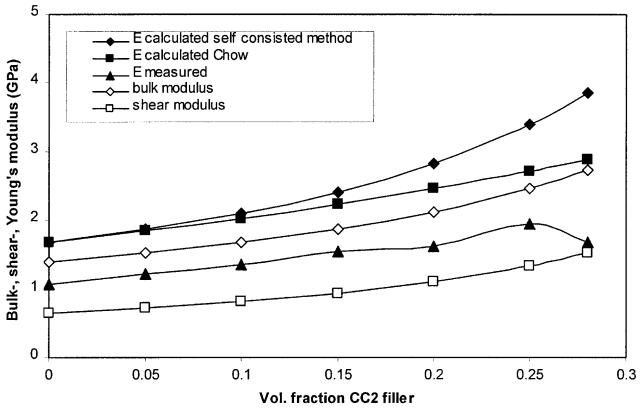

Fig. 21. Experimental measurements of the dependence of the Young's moduli compared with predictions made from the self consistent method and the Eshelby inclusion method.

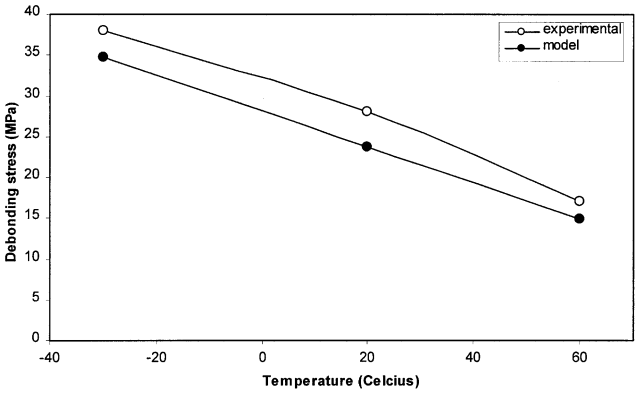

Fig. 22. Temperature dependence of the debonding stress: experiments and model prediction.

and −30°C. This is fully consistent with the temperature dependence of the elastic compliance s_{66} measured by Lin and Argon [14] in fully textured Nylon-6 in simple shear experiments. There is a 75% drop in the Young's modulus between 20°C and 60°C. This is attributed to a glass transition in the amorphous component occurring in the range of 300–310 K, in Nylon-6 having similar levels of water content as noted by Lin and Argon [14]. The enhancement of the modulus at 20°C with filler volume fraction reported in Tables 4 and 6 are compared in Fig. 21 with values calculated by the self consistent method [17] and by the Eshelby inclusion method of Chow [18]. In these calculations, explained in Appendix A, a shear modulus of 646 Mpa and a Poisson's ratio of 0.3 were used for unmodified nylon, based on the measurements of Lin and Argon [14]. These values predict an operationally required bulk modulus and a corresponding Young's modulus which were both about 30% higher than the values reported in Tables 4 and 6. The latter were lower presumably due to the high compliance of the tensile load train. The calculated trend of the dependence of E on the volume fractions c of filler parallels well the experimentally measured dependence, particularly with the Chow method.

4.2. Debonding of particles

As noted in Section 3, the initial linear response of the modified blends, particularly for larger volume fractions of filler particles, shows clearly observable breaks in the slope, changing from the expected stiffened behavior to below that of the unmodified nylon. This is attributed to the debonding of the particles from the matrix when the behavior of enhanced stiffness is replaced with the lower stiffness of a partially cavitated matrix. These debonding stresses appeared to be independent of filler volume fraction but dependent on temperature, as shown in Fig. 22. The dependence is nearly linear but with an increasing slope between 20°C and 60°C. A judicious extrapolation of the results would suggest that the debonding stress should vanish around 100°C. These all indicate that it is most likely that there is no real adhesion between particles and the matrix, but that the matrix has shrunk down around the particles by differential thermal contraction. Such thermal-misfit clamping can be readily verified both experimentally and theoretically. If the attachment of the particles to the matrix is a result of thermal clamping alone, the application of a tensile stress to the blend, somewhat exceeding the 'debonding' stress, will lower the modulus as described. If this response remains entirely in the elastic range, removal of the applied stress should revert the state reversibly to its initial clamped state, and a subsequent re-loading should reproduce a new response indistinguishable from the initial loading response. That this is indeed the case is demonstrated in Fig. 23 for a CC2 blend containing a volume fraction of 0.2 of particles. The solid curve shows the initial elastic response of the intact blend, with a clearly discernable kink at a load of roughly 1350 N, where 'debonding' occurs. The dotted curve represents the response to re-loading of the sample after unloading. The re-loading curve has an identical shape to the initital loading curve with, however, a slightly lowered level of the 'debonding' stress

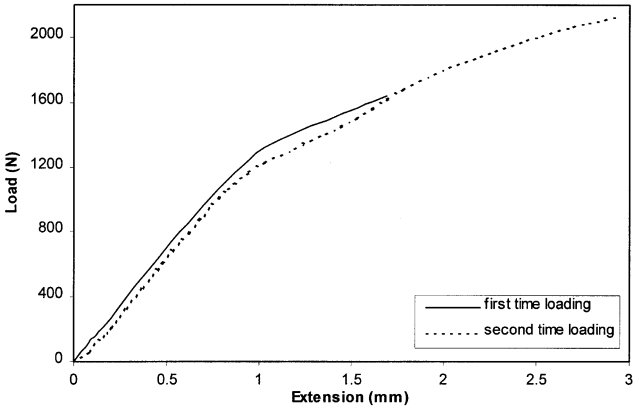

Fig. 23. Reversible particle debonding behavior. Solid curve gives initial response. Dotted curve gives response on re-loading.

that suggests that the closing of the gaps between the particles and the matrix is not completely reversible on unloading. Thus, the response of the modified blends is more in the nature of stress induced interfacial separation of pre-pressurized particles from the surrounding matrix that clamps down on them, rather than the actual debonding of adhered particles. A simple analytical development gives the clamping pressure p on a spherical particle of known bulk modulus K_p and volumetric coefficient of thermal expansion of γ_p administered by a matrix of composite shear modulus μ_c and composite volumetric coefficient of thermal expansion of γ_c giving [19],

$$p = \frac{(\gamma_p - \gamma_c)\Delta T K_p}{\left[1 + \frac{4\mu_c}{3K_p}\right]} \tag{2}$$

where γ_c and μ_c of the composite matrix are obtainable from supporting developments that are summarized in Appendix B. To determine the debonding stress σ_{db}, as it manifests itself on the stress strain curve, it is necessary to determine the mean normal stress σ_m induced by the applied tensile stress in the particle. Particle separation should then occur when the induced σ_m neutralizes p. This finally results in an expression for σ_{db} given as (Appendix B):

$$\sigma_{db} = \frac{3(\gamma_p - \gamma_c)\Delta T K_p}{\left[1 + \frac{4\mu_c}{3K_p}\right]} \times \left[1 + \frac{2(1 - 4\nu + \nu^2)\left(\frac{K_p}{K_c} - 1\right)}{(1+\nu)\left[2(1-2\nu) + (1+\nu)\left(\frac{K_p}{K_c}\right)\right]}\right]^{-1} \tag{3}$$

This calculated σ_{db} stress is also plotted in Fig. 22 for the various material constants given in Appendix B. The calculated dependence is slightly different from the measured one but in overall outline supports the interpretation.

4.3. The features of the 'engineering' stress strain curves of unmodified nylon

Figs. 1, 3 and 4 show the initial yield behavior, the necking, stretching and hardening of both the unmodified and particle-modified-blends of nylon. These curves show a systematic decrease of the initial yield stress with increasing volume fraction c of particles. To appreciate the intrinsic behavior of the nylon we examine first the features of the unmodified material in tension at 20°C, shown in Fig. 1a and b and also in Fig. 2. The curves in Fig. 1a and b show a very prominent yield phenomenon where global plastic response is initiated. It is followed by a short plateau with slightly decreasing plastic resistance and a subsequent sharp drop to a lower level representing the necking and stretching response of the bars. The yield drops and the necking are closely spaced but still well separated. As is well known, the true-stress/true-strain curves of polymers, whether glassy or semi-crystalline, away from their respective glass transition temperatures, will show a well defined elastic to plastic transition, followed by a hardening behavior which will show a progressively increasing slope and, if fracture does not interfene, and eventual 'locking' behaviour when stretched molecules become substantially aligned by plastic flow and their stiff backbone stretching behavior sets in. In many glassy polymers this behavior is replaced globally by crazing, where, however, the intrinsic hardening behavior is still present in the craze fibrils. The mechanism of hardening by molecular alignment in glassy polymers differs fundamentally from that in semi-crystalline polymers, where in the latter, crystallographic slip processes in the crystalline lamellae become dominant. These differences have been extensively discussed in the literature (see e.g. Refs. [20–26]) and are not a subject for expansion here. The relevance of these observations are that in a polymer, without a specific yield phenomenon, at a temperature significantly below T_g, the tensile deformation becomes unstable when the true flow stress exceeds the hardening rate, i.e. where $(\sigma - (d\sigma/d\epsilon)) > 0$. There necking and localization of deformation starts and produces a characteristic stretch-induced area reduction that is (erroniously) referred to as the 'natural draw ratio'. The stretched material then reaches a further point along the true-stress/true-strain curve where $(\sigma - (d\sigma/d\epsilon)) < 0$, where deformation is stabilized again. Then, if premature fracture does not intervene, the tensile bar becomes fully converted under constant load into a fully stretched form as one or both of the shoulders propagate along the length of the bar until grip regions of larger cross sectional area are reached. This point (B) on the stress strain curve where stability of stretch is again attained, is characterized fully by the loaded extension curve, as given by e.g. Fig. 1a. The flow stress σ_s and the critical strain hardening rate $(d\sigma/d\epsilon)_s$ and the true strain ϵ_s for this point where stability is regained are:

$$\sigma_s = \left(\frac{d\sigma}{d\epsilon}\right)_s = \frac{P_{lp}}{A_n} \tag{4a}$$

$$\epsilon_s = \ell n \frac{A_0}{A_n} \tag{4b}$$

In Eqs. (4a) and (4b) P_{lp} is the reduced stretching load at the lower plateau, A_n the cross sectional area of the stretched neck, A_0 the initial cross sectional area of the unstretched gage section of the specimen. The point where necking is initiated, in turn, is directly given by the load-extension curve where the upper plateau load P and the inception strain ϵ_u can be taken where P_{up} begins to show a downward trend. Thus, for the point (A) of iniation of a neck the

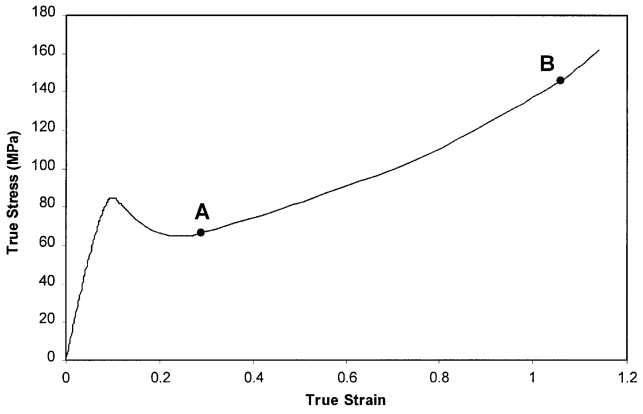

Fig. 24. A tensile true-stress/true-strain curve for unmodified Nylon-6.

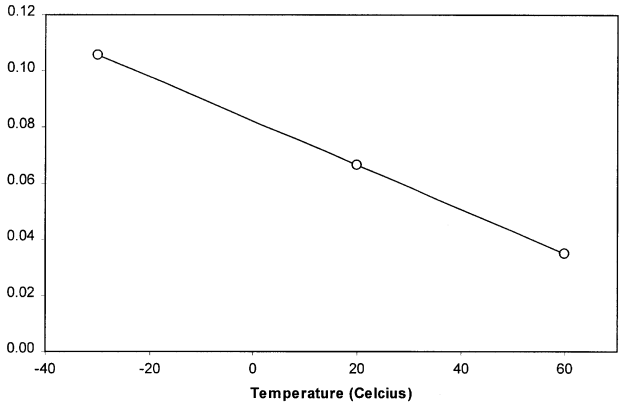

Fig. 25. The temperature dependence of the yield stress normalized with the appropriate Young's modulus.

conditions should be:

$$\sigma_u = \left(\frac{d\sigma}{d\epsilon}\right)_u = \frac{P_{up}}{A_0} \tag{5a}$$

$$\epsilon(= \text{as determined from the curve}). \tag{5b}$$

In polymers exhibiting a well defined yield phenomenon as, is prominently present in the experiments at 20°C, this can be taken directly as reflecting the behaviour of the true-stress/true-strain curve. Thus, points (A) and (B) as well as the form of the yield phenomenon as given in the load-extension curves of the unmodified nylon of Fig. 1a or b can be used to create the true-stress/true-strain curve of the latter at room temperature. This curve is shown in Fig. 24. The portions of the curve between points A and B, (with their given locations and slopes), has been 'faired-in'. The shape of the true-stress/true-strain curve of Fig. 24 is quite consistent with measured as well as simulated behaviour curves for textured HDPE [25,27].

There are important differences between the curves at 20°C and those at 60°C as well as those at −30°C. At 60°C the curves show neither a yield phenomenon nor localization by necking. Both of these effects are attributable to a glass transition in the amorphous component between 300–310 K. This lowers the plastic resistance to below the hardening rate at all strains, making $(\sigma - (d\sigma/d\epsilon)) < 0$ everywhere. Since at this temperature deformation will start in the amorphous component where there will be little resistance to an onset of plastic shear, this results in an absence of a yield phenomenon. The origin of the different behavior at −30°C is less clear. Here too there is no yield phenomenon, where the smooth onset of plastic response might be a consequence of the very substantial thermal expansion anisotropy in the crystalline component of the monoclinic Nylon-6 crystal lamellae [28]. This thermal expansion anisotropy could initiate random local plastic flow between ordered domains-well before global plastic flow could be achieved. The unmodified nylon samples, however, exhibit a very pronounced localization by necking at −30°C. We note here in passing, that these considerations also apply to the particle modified blends where both the flow stress and the strain hardening rate are decreased in the same proportion, resulting in no dependence on the stable stretching strain (natural draw ratio). The observed reduction of the strain to fracture in the blends is a direct result of embrittling particles of super-critical size as discussed in Section 4.6.

The yield stress of unmodified Nylon-6 is governed by fundamental processes of shear resistance in the amorphous and the crystalline components in a complex way. In any case the relevant mechanisms must involve local elastic interactions at the molecular segment level. Thus, the temperature dependence of these mechanisms are related both to the elastic properties and to their anharmonic connection to temperature as well as to the thermally assisted isostructural local relaxation processes that should reflect a genuine Arrhenius type temperature dependence. To separate the anharmonic from the Arrhenius contribution it is usual practice to represent the yield stress in units of the local elastic constant at the given temperature. Such a plot of Y/E is given in Fig. 25 for the range between −30 and 60°C. Instructively, the ratio is a continuously decreasing function, taking no note of the prominent glass transition in the range of 25–35°C, since this transition affects the yield strength Y and the Young's modulus in the same way.

4.4. Yield behavior of modified blends

Examination of the yield behavior of modified blends at 20°C shown in Fig. 1a and b indicate a systematic decrease of the yield stress with increasing volume fraction of filler particles. This gives further clear evidence that in all blends particle separation from the deforming matrix had occurred during the initial loading portion of the deformation response. Thus, if it can be assumed that at the yield point the internal cavitation was complete, and that the particles were substantially separated from the matrix, so that the blends can be considered to have had porosities nearly

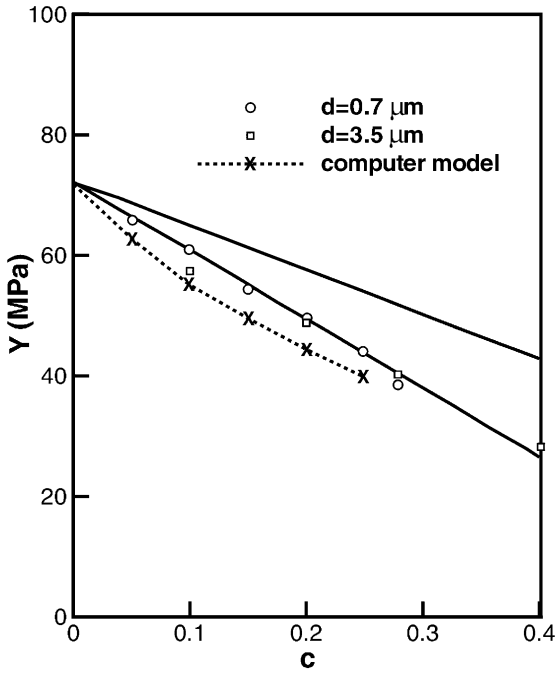

Fig. 26. Dependence of the yield stress on particle concentration: experimental values, upper bound calculations and computer model results.

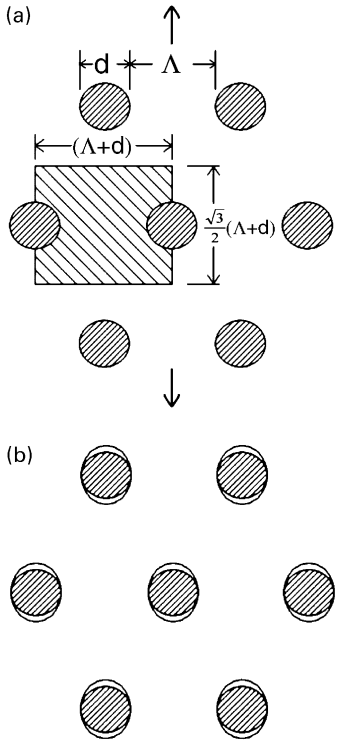

Fig. 27. A 2-D model of the CC particle distributions in the matrix: (a) before deformation, (b) after debonding during loading to yield stress showing particle separation at the poles.

equal to the initial particle volume fraction, the yield stress should decrease nearly linearly with increasing volume fraction of filler. Such behavior represented by an upper bound model for plastic non-hardening behavior is plotted in Fig. 26, together with the actual experimentally determined yield strengths for the CC2 and CC1 blends over their entire range. The experimental behavior pattern also obeys a linear dependence, but with a larger slope indicating that the actual behavior develops with a lower plastic resistance, obeying a dependence of $Y = Y_0(1 - 1.62c)$. This dependence compares reasonably well with a micromechanical computer model of Danielsson et al. [29] the results of which are also plotted in Fig. 26.

Examination of the near-post-yield behavior of the blends and comparison with behavior of unmodified nylon shows a significant relatively stable strain softening behavior before localization sets-in to form a neck. In the unmodified nylon simple considerations give the slope of the load-extension curve as

$$\frac{\mathrm{d}P}{\mathrm{d}\ell} = \frac{P}{\ell}\left(\frac{1}{\sigma}\frac{\mathrm{d}\sigma}{\mathrm{d}\epsilon} - 1\right) \tag{6}$$

In the absence of a yield phenomenon the term in parenthesis in Eq. (6) should be positive. When a yield phenomenon is present, however, and the strain softening range of the yield phenomenon extends over to the point of initiation of the necking instability, as the stress strain curve of Fig. 24 suggests, the term in parenthesis can be negative over a range of strain.

For the corresponding process in the modified blends, again a similar simple analysis gives:

$$\frac{\mathrm{d}P}{\mathrm{d}\ell} = \frac{P}{\ell}\left(\frac{1}{\sigma}\frac{\mathrm{d}\sigma}{\mathrm{d}\epsilon} - 1\right) - 2\frac{P}{\ell(1-c)}\frac{\mathrm{d}c}{\mathrm{d}\epsilon}, \tag{7}$$

with the second term resulting from the plastic cavity expansion process with strain. This would then result in a stronger quasi-stable strain softening behavior in the modified blends as some of the curves in Fig. 1a suggest.

4.5. Plastic ligament stretch and its role in toughness

The plastic cavity expansion in Nylon-6 with local regions surrounding the cavities having anisotropic plastic resistance, as the studies of Muratoğlu et al. [7,8] suggest, have been modeled by Tzika et al. [30], using a fully developed elastic-plastic finite element approach, taking the local deformations to equivalent strain levels of 0.18. For our purpose to develop some understanding of the toughening behavior, to very much larger strains, we relate the behavior to the plastic stretching response of a local representative material ligament which will become also useful in characterizing ultimate rupture response in a time and rate dependent framework.

Thus, consider a 2-D idealization of the particle-modified-blend as a set of parallel rigid cylinders of diameter d in a hexagonal packing, with nearest interparticle spacing, Λ, as depicted in Fig. 27a. This, upon particle

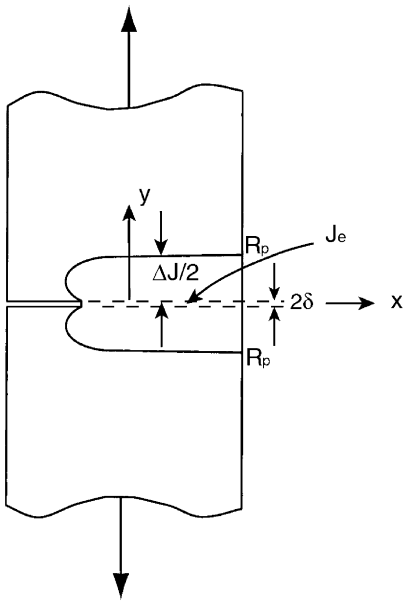

Fig. 28. Sketch of the whitened zones of the SECP specimens.

separation produces a regularly porous solid, stretched in the vertical direction as depicted in Fig. 27b. We identify the hour-glass shaped region as the representative matrix ligament material that is a candidate to stretch plastically and absorb energy. In this representation the volume fraction c of particles that gives rise to the same level of initial porosity upon particle separation is

$$c = \frac{\pi}{2\sqrt{3}} \frac{1}{\left(1 + \frac{\Lambda}{d}\right)^2} \tag{8}$$

while the volume V of the representative ligament is

$$V = \frac{\pi d^2}{4} \frac{(1-c)}{c} \tag{9}$$

The inelastic constitutive deformation resistance of this representative matrix ligament will have a shape given in Fig. 24 with a monotonically steepening upturn of resistance due to textural hardening in tensile extension. This form is similar to the hardening behavior exhibited by flexible chain glassy polymers albeit based on a very different mechanism. In the latter case this behavior can be represented by the formalisms of non-Gaussian rubber elasticity, as has been demonstrated by a number of investigators [20–24]. Even though the basic physical mechanisms of the hardening behavior in the semi-crystalline nylon and that in glassy polymers are radically different, for purely formal purposes of analysis we adopt the well developed analytical formalism of the glassy polymers as described, e.g. by Boyce and Arruda [24]. As we demonstrate in Appendix C this development leads to a relatively simple expression for the plastic work of fracture, W_p, of a ligament, per unit thickness as:

$$W_p \cong \frac{\pi d^2 Y_0}{4}\left(\frac{1-c}{c}\right)\ell n\lambda_n \tag{10}$$

Finally, this gives for the essential work of fracture J_e on the plane of separation, again per unit thickness:

$$J_e = \left(\frac{\sqrt{3}\pi}{8}\right)^{\frac{1}{2}}\left(\frac{(1-c)}{\sqrt{c}}\right)Y_0 d\ell n\lambda_n. \tag{11}$$

To apply this expression to determine an estimate of overall J that can be compared with the measured fracture toughness J of the SECP specimens, it is necessary to evaluate the accompanying dissipated plastic work in deforming the two flanks adjacent to the fracture surface, as outlined in Fig. 28. While the layer of thickness

$$2\delta = \frac{\sqrt{3}d}{2}\left(\frac{\pi}{2\sqrt{3}c}\right)^{\frac{1}{2}} \tag{12}$$

ruptures along the median plane of separation to result in the essential work of fracture given in Eq. (11) above, similar ligament stretching processes of decreasing intensity take place in the surrounding zones of thickness R_p. The additional contributions ΔJ to the work of fracture can be obtained readily through standard procedures of non-linear fracture mechanics and result in an overall fracture toughness of: (developed in Appendix C)

$$J = J_e\left(1 + 2\,\ell n\left(\frac{\epsilon_f}{\epsilon_0}\right)\right), \tag{13}$$

where $\epsilon_f = \ell n\lambda_n$ is the ultimate strain of ligament fracture in the low strain rate limit and ϵ_0 is the elastic strain at yield.

Considering as a check, the nylon/CC2 blend with 0.05 volume fraction of particles having matrix plastic resistance $Y_0 = 71.7$ MPa, as indicated in Table 4, a locking stretch $\lambda_n = 5.0$ as is suggested from the fractographs of Fig. 10 and $\epsilon_0 = 3.9 \times 10^{-3}$ as given earlier, we determine $J_e = 126\ \mathrm{J/m^2}$ and $J = 1.9\ \mathrm{kJ/m^2}$ with a whitened zone of thickness $2R_p = 1.1$ mm. The actualy measured value of J was $9.42\ \mathrm{kJ/m^2}$ with a considerably thicker surrounding whitened zone of the order of 2–3 mm. This indicates that the geometry of the chosen SECP samples were less than ideal, and in their plane stress mode of fracture underwent considerably larger levels of surrounding whitening to account for the factor of 4.86 difference between the measured and the estimated level of fracture toughness.

The fracture toughness of the nylon/CC2 particle blends with volume fractions larger than 0.05 can be calculated also readily from Eqs. (11) and (13). These values, normalized with the toughness of the blend having 0.05 volume fraction of particles are shown in Fig. 29 by the solid curve while the experimental results are shown with the open circles. The trend in decreasing toughness is reasonably well predicted by the model.

We note that the load-displacement plot for the unmodified nylon shown in Fig. 7b has a much more brittle appearance in comparison with the responses of the blends with 0.05 and 0.1 volume fraction of particle filler. This gives the reason why the fracture toughness of the unmodified nylon

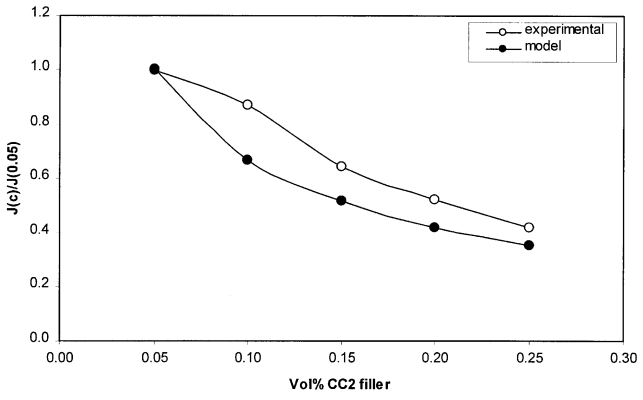

Fig. 29. Calculated normalized fracture toughness compared with experiments.

is 30% lower than that of the blend with 0.05 particle concentration as shown in Fig. 9a. This behavior furnishes a clear demonstration of the toughening strategy based on particle modification. While there is little to impede the propagation of a crack in the brittle unmodified nylon, in the pre-cavitated cellular material of the blend with 0.05 particle concentration the effectively lowered local plastic resistance results in dramatic crack blunting followed by the development of a large local ligament sketching response before the stretched ligaments eventually rupture.

The measured fracture toughness of the nylon/CC1 blends shown in Fig. 9b are considerably lower than those of the CC2 particle blends while much higher toughnesses are predicted by Eq. (11). The reason for this poor behavior is partly indicated by the fractographs of Fig. 12a and b, which indicate that the wider particle size distribution and the severely angular shapes of these larger particles have sharply curtailed the development of a quasi-regularly porous matrix required for the needed stretching of the ligaments.

We note that on SECP specimen fracture toughnesses are fully a factor of 264 larger than those measured by Maratoğlu et al. [9] on a rubber modified Nylon-6 blend with rubber particle sizes of 0.32 μm and volume fraction of 0.2 in special elongated double cantilever beam samples with side grooves, developing considerably higher levels of triaxiality. All these effects will result in very significant reduction in fractures resistence. Rescaling the Muratoğlu et al. [9] measurements can be shown to result in good agreement with our measurements in the cavitated CC2 particle blends.

4.6. Inclusions and embrittlement

As has been demonstrated in Fig. 11a–d, uncharacteristically large inclusions, often resulting from the clustering of particles, as has been the case in the majority of observations, will initiate super-critical crack-like flaws that can propagate in a brittle manner before the rest of the more uniformly cavitated microstructures can undergo plastic stretching. To evaluate the flaw sensitivity of the particle modified blends, we use the plane strain fracture toughness measurements of Muratoğlu et al. [9], already referred to above. There measured plane strain fracture toughness was $J = 34.8\ \mathrm{J/m^2}$ in a modified Nylon-66 blend containing a volume fraction of 0.2 of cavitated particles of 0.32 μm diameter.[1] Considering triggering local brittle response during flow, the critical half length a of a crack-like flaw can be estimated from

$$a = \frac{1}{\pi}\frac{JE}{(1-\nu^2)(1-c)^2(Y_0)^2} \tag{14}$$

For $E = 1.68\ \mathrm{GPa}$, $Y_0 = 71.7\ \mathrm{MPa}$ and $c = 0.2$ this would give a critical crack half length ranging from 4–6 μm, depending on filler volume fraction (0.05–0.2) at the above mentioned plastic resistance level. Examination of fracture surfaces of both slow tension bars and Izod impact bars have revealed numerous particle clusters larger than this estimate in the CC2 particle-modified-blends, each showing evidence of embrittling effects. Thus, it is clear that elimination or at least radical reduction of such particle clustering during material preparation should help the development of very attractive levels of toughness in the CC2 particle-modified-blends in all but impact response. The toughenability of the blends with the much larger CC1 particles of sizes ranging up to 10 μm, or larger, with their severe, sharp corners, is clearly highly doubtful. The poor results in slow tension and in toughness measurements with SECP experiments attest to this fact that in these blends many of the particles already act as super-critical flaws. The very poor Izod results of both blends have a different origin in the drastically hastened facture behavior of the matrix ligaments due to both a high strain rate sensitivity of the plastic resistance of nylon and the development of a substantial negative pressure, as we will discuss in Sections 4.7 and 4.8 below.

4.7. Izod bending impact toughness

The Izod impact energies measured for all blends at 20°C show a uniformly disappointing behavior. For the CC2 particle-modified-blends which incorporated well shaped quasi-spherical particles with consistent trends in stress strain experiments, impact experiments showed a modest increase in energy over the unmodified nylon, from 0.07 kJ/m to a peak increase to 0.13 kJ/m for the blend with 0.15 filler particle concentration, with the 'far-end' samples showing a slight improvement over the 'gate end' samples. Fractography revealed no plastic ligament-stretching-response but only a spongy-appearing terraced brittle response. There was clear evidence in every case that the particles had debonded prior to fracture and that the poor

[1] In the evaluation of their fracture toughness measurements Muratoğlu et al. [9] used a tensile plastic resistance of 31.6 MPa instead of a more appropriate value of 71.7 MPa. If this correction is made for their measurements, the above cited value of 34.8 J/m^2 is obtained.

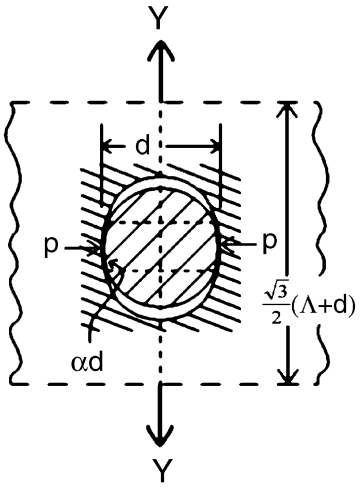

Fig. 30. Sketch of incompletely separated particle, producing triaxial tensile stress.

behavior could not be attributed to a failure in particle debonding. This fact was verified by stretching a series of tensile bars of blends, with previously studied volume fractions to just over the yield phenomenon to achieve particle debonding. These stretched tensile bars were then re-machined into Izod bars and tested in impact.

The measured impact energies of these pre-cavitated bars are also shown in Fig. 5a by the white columns. With the exception of the unmodified material which had not been pre-cavitated but merely pre-stretched and showed a two-level fracture behavior in which the upper level exceeded the earlier measurement, the Izod energies of the pre-cavitated samples were uniformly lower demonstrating both that the pre-stretching had compromised some toughness potential and that the lower levels of impact energy could not be attributed to a failure of particle debonding. The two-level behavior of the unmodified nylon correlated with the presence or absence of cracking bifurcation. In samples with initial crack bifurcation the toughness was nearly twice as high as in those which did not show this effect. While this improved toughness could be attributed to the mutual shielding of the two cracks, the cause for such apparently random bifurcation behavior was not clear.

When the present results with CC2 particle-modified-blends are compared with the earlier results of rubber modified blends studied by Muratoğlu et al. which incorporated very similar levels of particle volume fractions, processed under closely similar conditions and showed quite attractive levels of Izod impact energies, the difference in behavior stood out dramatically. In both cases the particles had either cavitated (rubber) or debonded (CC2 particles), the nylon matrix was identical and the increase in matrix plastic resistance due to the substantial increase in strain rate resulting from impact conditions (by an estimated factor of 10^6 or more) above the tension experiment was the same for both types of blends. Thus, it is necessary to attribute the very poor behavior of the CC2 particle-modified-blends to another cause such as to the development of a triaxial tensile stress caused by the interference of the rigid particles with the stretching of the matrix ligaments.

We imagine the effect to arise from the failure of the particles to fully separate from the matrix in the critical early stages of impact as depicted in Fig. 30 where the particles are shown to maintain contact over an arc length of αd. Such particles then act as plastic indenters on the matrix cavity surface and develop an indentation pressure that we take as βY_0 with β being considered to be between a factor of 2 and 3. This effect would produce a lateral compressive force on all partially debonded particles, in the early phases of impact response. By equilibrium a 2-D negative pressure in the polymer matrix should develop. As we demonstrate in Appendix D this would give rise to a triaxial tensile stress (a 3-D negative pressure) of

$$\sigma_m = 0.8\alpha\beta Y_0\sqrt{c}. \tag{15}$$

Thus, e.g. taking $\alpha = 0.3$, $\beta = 2.5$ and a volume fraction as 0.05 we would find a triaxial tensile stress of $0.135Y_0$ which elevates the tensile stress on the stretching ligaments by this amount and serves to hasten ligament rupture by chain scission.[2] For a volume fraction 0.2 of reinforcing particles the effect would double.

Thus, we attribute the brittle response of the CC2 particle-modified-blends to this additional triaxial tensile stress in the matrix, over and above the elevation of the plastic resistance of the matrix due to the increased strain rate of the impact condition.

4.8. Time dependent fracture of matrix ligaments and its role in toughanability

In what we have reported we found dramatic toughening effects in Nylon-6 blends with CC2 particles of diameter 0.7 μm, in slow tension experiments and in SECP experiments where in the latter fracture toughnesses of 9.24 kJ/m^2 were reported. In all instances, including in the Izod impact experiments there was clear evidence that particle separation had occurred well before initiation of plastic flow or fracture. Nevertheless, the Izod impact energies were disappointingly low. These energies were for unmodified nylon 0.07 kJ/m and in the best case with a volume fraction of particle of 0.15, only 0.13 kJ/m. In all instances fractography indicated brittle propagation of cracks with nearly no ligament stretching that was characteristic of the slow experiments. While comparison of our findings with the experiments of Muratoğlu et al. on rubber modified blends leaves a number of unanswered questions, it now appears to be very likely that the disappointing behavior is not entirely attributable to the embrittling effect of the high concentration of large clusters of particles but must reside also to a

[2] Clearly, the choice for β is an overestimate since the resistance to plastic flow in a direction normal to the principal direction of plastic deformation should be quite considerably less.

large measure in the intrinsic time dependent fracture of stretched (or stretching) nylon ligaments. We base this possibility on a very detailed set of experiments on diluent induced toughening of PS blends with low molecular weight liquid PB diluent that resulted in dramatic plastic-flow-induced toughening of PS as has been described by Qin et al. [31]. A unifying finding of these experiments, carried out with PB diluents of different molecular microstructure and volume fraction, at different temperatures and strain rates was the time dependent fracture of stretched PS fibrils in the craze matter. In that study all these effects could be represented by a universal rate dependent fracture relation of stretched PS ligaments, giving the time t_f to fracture under a constant craze stress σ at a constant temperature T, to be in a form of

$$\frac{\sigma}{\sigma_0} + \frac{T_0}{\theta} = 1. \tag{16}$$

where σ_0 and T_0 are material dependent intrinsic normalization parameters, and where

$$\theta = T\mathcal{L}n(\nu t_f) \tag{17}$$

is a combined temperature, time-to-fracture, t_f, parameter with, ν, being a frequency factor in the range of 10^{12}–10^{13} s^{-1}. Translating the formalism from craze stress to fibril or ligament stress through the volume fraction of fibrils in crazes, the universal relationship for the time to fracture t_f becomes,

$$t_f = \frac{1}{\nu}\left(\frac{\tilde{\sigma}}{\sigma}\right)^n \tag{18}$$

where for PS, $\tilde{\sigma} = 4.8$ GPa and $T_0 = 2200$ K with $n = T_0/T$ and $\nu = 10^{12}$ s^{-1}.

Qin et al. demonstrated that with this relationship, obtained from craze flow experiment under tensile stretching, an increase of strain rate by a factor 10^6, the resulting elevation of the plastic resistance σ of the craze fibrils would reduce the very attractive tensile toughnesses (area under the stress–strain curve) to vanishing levels, accounting for the very disappointing performances of the diluent-modified-blends under near impact conditions.

Extension of this time dependent fracture behavior to the very similar response of the nylon blends where the ligaments continue to stretch and experience increasing strains is readily possible by introducing the notion of accumulation of chain scission damage given by a damage function ξ which is defined in incremental form as

$$d\xi = \frac{dt}{t_{f0}} \tag{19}$$

where t_{f0} is the time to fracture under constant stress, as defined in Eq. (18). There is a large body of experimental information on the evolution of chain-scission-damage in stressed polymers reported in the past by Zhurkov and co-workers [32] and by Peterlin [33], leading to eventual fracture; that support this proposition.

Then, under a history of increasing stress $\sigma(t)$, the time to fracture t_f at a given temperature T should result when $\xi \rightarrow 1.0$. Thus, where

$$\nu \int_0^{t_f} \left(\frac{\sigma(t)}{\tilde{\sigma}}\right)^n \mathrm{d}t = 1.0. \tag{20}$$

In the plastic deformation of stretching ligaments, $\sigma(t)$, represents the current level of plastic resistance which depends on both T and $\dot{\epsilon}$. Under these conditions the fracture of ligaments should occur in an experiment at constant temperature and under constant applied strain rate $\dot{\epsilon}$ when

$$\frac{\nu}{\dot{\epsilon}} \int_0^{\epsilon_f} \left(\frac{\sigma(\dot{\epsilon}, \epsilon, T}{\tilde{\sigma}}\right)^n \mathrm{d}\epsilon = 1.0 \tag{21}$$

In the experiments of Qin et al. [31] where the required material information was available it was demonstrated that brittle behavior would result through the severe reduction of ϵ_f with $\dot{\epsilon}$, increasing by a factor of 10^5. How these same considerations apply to the nylon blends discussed here through an increase of strain rate from slow tension to Izod impact (an increase by a factor of 10^6–10^7) will be discussed in a separate communication by Tunca et al. [34].

4.9. General considerations of toughenability of brittle polymers

In the present experiments we have demonstrated that there is a definite and attractive potential for toughening of unmodified nylon with rigid, quasi-spherical $CaCO_3$ particles which are attached to the nylon matrix by only a thermal misfit induced clamping effect. Izod impact experiments show that unmodified nylon fractures in a very brittle manner with an energy absorption of only 0.07 kJ/m. A more definitive SECP experiment at an imposed velocity of 8.3×10^{-5} m/s. (rather than 4.8 m/s at impact) results in a fracture toughness of 4.0 kJ/m^2. Incorporation of a volume fraction 0.05 of $CaCO_3$ particles that separate from the matrix before flow, results in a decrease of the tensile flow stress by 9% and an increase in the fracture toughness to 5.8 kJ/m^2 and show massive accompanying whitening in layers adjacent to the crack plane. These are positive findings. In Izod impact experiments, however, only brittle behavior was found with Izod energies no larger than 0.13 kJ/m, for particle volume fractions of 0.15, indicating at best only a modest improvement by a factor of 1.85 over unmodified nylon, by a crack deflection toughening mechanism [36], with no evidence of any matrix plastic ligament stretching. While a high incidence of large particle clusters has definitely contributed to the brittle response the major cause of the embrittlement is attributed to the already very high flow stress of unmodified nylon at 72 MPa and its substantial elevation due to the increased strain rate under impact conditions which we propose must result in the hastening of ligament facture by chain scission.

Comparing the present results with those of the rubber-modified Nylon-6 blends of Muratoğlu et al. [8,16] where

quite attractive toughness levels were reported in Izod impact experiments, it is clear that the elevation of plastic resistance due to increased strain rate can not be the sole cause for brittle behavior.[3] In Section 4.7 we have proposed that the interference of the separated rigid particles from the matrix must result in the development of substantial levels of a triaxial tensile stress, at least in the critical early stages of incipient plastic response in the matrix. Such triaxial tensile stresses would promote plastic cavity expansion and as a result should relax. Nevertheless, before such relaxation can develop by plastic cavity expansion, the triaxial stress will elevate further the stresses acting on the ligaments, over and above the stress rise due to the increased plastic resistance resulting from the high strain rates of the impact condition. It is proposed that this effect of the particles negates their benefitial effect of lowering the plastic resistance of the modified nylon by the establishment of the quasi regular porosity. Clearly, in this quest to nurture a plastic response, the over abundance of super-critical particle clusters is quite detrimental in repeatedly-triggering brittle response. Thus, in this analysis the comparative benefitial influences on toughening of rubber particles become clearer. First, in the rheology of flow processing of modified polymer blends achieving quasi regular dispersion of rubbery domains of appropriate size ranges, well under the critical flaw sizes, is relatively more readily possible than proper dispersion of quasi-spherical rigid particles. The findings of the present study indicate that rigid particles in the submicron size range such as the 0.7 μm diameter $CaCO_3$ particles, are very difficult to quasi-regularly disperse against the various tendencies that result in their clustering by flow channeling during processing and by bonding together. Thus, in the nylon blends with their already high plastic resistances in the 70–80 MPa range the critical flaw sizes that trigger brittle behavior are much more readily reached with inorganic filler particles and their tendencies to cluster, than with the alternative approach of achieving the quasi-regular porosities with cavitating rubber particles.

The above consideration becomes even more instructive if the results with nylon are compared with those of the toughening studies of Bartczak et al. of HDPE with either rubbery particles [10] or $CaCO_3$ particles [11]. We note that the toughenability of HDPE to a large measure is attributable to its relatively low plastic resistance of 25 MPa at 20°C due primarily to the quite low T_g of it's amorphous component.

Finally, we return to the role of the critical matrix ligament dimension criterion in obtaining toughness jumps in readily crystallizable semi-crystalline polymers, such as nylon and HDPE, for which the occurrence of preferentially crystalized layers around particles had been demonstrated conclusively by both Muratoğlu et al. [7] and by Bartczak et al. [10,11,37]. In the present experiments the results on the depression of yield stress due to both CC2 and CC1 particles, shown in Fig. 26 indicate no difference between the two types of particles. We attribute this to be fact that with the widespread particle clustering problem the interparticle ligaments were in all probability above the required dimension of 0.3 μm for the blends with the 0.7 μm diameter CC2 particles with volume fractions under 0.2, and certainly well above with the 3.5 μm diameter CC1 particles at all volume fractions.[4] Our present results show that in addition to a critical ligament dimension that can affect toughening the critical flaw size that triggers brittle behavior is of equal importance in all cases as we have demonstrated.

We note in this connection that the window of opportunity is quite narrow in toughening polymers all of which exhibit intrinsic brittleness. In most polymers the separation between stresses to initiate plastic flow and those that produce fracture by chain scission or inter-molecular separation is well within a factor of 10 (unlike in metals where the range is often a factor of 10^3). This makes toughening of polymers with already high flow stresses such as nylon rather more demanding than those such as HDPE where the range is more comfortably large.

5. Conclusions

Most, if not all, unmodified polymers are intrinsically brittle, exhibiting low resistances to crack growth at low temperatures, and high rates of loading, including notched impact experiments.

When modified with well dispersed compliant or rigid equi-axed heterogeneities that either cavitate or debond before plastic flow is initiated, such polymers are rendered to have a cellular microstructure which promotes ligament stretch and tough behavior in an expanded range of temperature and loading rate.

Such toughenability has been studied in blends of polyamide-6 (Nylon-6) modified by $CaCO_3$ (CC) particles of both 0.7 μm and 3.5 μm average diameter. The following was noted.

[3] We note here that Muratoğlu et al. [8,16] have reported Izod impact energies of rubber-particle-modified nylon blends in two publications. While their reported values in Ref. [8] are quite consistent with ours for unmodified nylon, those reported in Ref. [16] are all a factor of 10 too high due to a slip-up in data manipulation. This is being corrected by a corrigendum to be published in the original journal [35].

[4] Paranthetically, we note that the relationship given for the critical ligament dimension by previous investigators [8,10,11] as $\Lambda = d[(\pi/6c)^{1/3} - 1]$ is inconsistent with the principles of stereological sampling of randomly distributed equiaxed heterogeneities by planar sections in which the area fraction on the sampling plane represents the volume fraction. On the basis of this, the correct relation should be $\Lambda = d[(\pi/2\sqrt{3}c)^{1/2} - 1]$. Nevertheless, since all previous authors have based their degree of success or failure on the improper expression, we have also considered the incorrect form in comparing our results with theirs. However, if the critical crystallization distance can be measured separately by independent means [37], its relation to the toughening potential in blends must use the proper sampling relation, based on well established principles of stereology [38].

The CC particles exhibit no chemical adhesion to the matrix but are held-in place only by a thermal-misfit induced pressure which in, all cases is overcome in tensile loading before yield. Incorporation of CC particles systematically lowers the yield stress linearly with increasing volume fraction of particles. While this should have resulted in a benefitial increase in strain to fracture this was not the case, in the modified blends due to premature fracture initiation from a ubiquitous population of large particle clusters which upon separation acted as supercritical flaws, triggering brittle response.

All Izod impact response was brittle at room temperature, with all fracture surfaces of the modified blends exhibiting a spongy appearance resulting from cavitation preceding plastic flow, but the inability of such flow to be initiated. A small increase of Izod toughness with increasing particle concentration resulting in a rough terrace type fracture was attributed to a crack-deflection effect.

The poor Izod impact performance of the modified blends was attributable to a combination of the high strain rate-induced-elevation of the plastic resistance and the development of a triaxial tensile stress due to incomplete separation of the rigid particles from the matrix in the crucial early stages of the impending matrix ligament stretching process. The latter effect, which was absent in the rubber modified Nylon-6 blends of Muratoğlu et al. [8,16], was responsible for their reported attractive Izod toughness levels.

Comparison of findings in the present study with those of others indicates that since the mechanics criteria of flow and the physics of rupture by chain-scission are relatively unalterable, polymers with reduced plastic resistance such as HDPE at room temperature have a better potential for further toughening in comparison with those such as the polyamides with an already high plastic resistance. In this quest reduction of plastic resistance due to preferrentially crystallized layers, present around particles, play a benefitial role.

Acknowledgements

This research was supported by the NSF MRSEC program through the Center for Materials Science and Engineering at MIT from Grant DMR-98-08941. We acknowledge with thanks receiving some experimental information from Dr Z. Bartczak related to his earlier study of 1997. MWLW acknowledges the encouragement of Professor M.A.J. Michels of the Technische Universiteit Eindhoven.

Appendix A. Elastic moduli of blends

The elastic moduli, i.e. the shear moduli, μ_c, and the bulk moduli, K_c of the nylon/CC blends can be calculated readily if the moduli for the components, i.e. nylon and calcite are known. Two prominent methods that lend themselves to the equiaxed isotropic fillers and matrix polymers, are the self consistent method as formulated by Budiansky [17] and the Eshelby inclusion method of Chow [18]. In the first method the composite shear modulus μ_c and bulk modulus K_c are calculated from the simultaneous solution of 5 equations by numerical techniques. These are

$$\frac{(1-c)}{1+\beta^*\left(\frac{\mu_m}{\mu_c}-1\right)}=1 \quad \text{and} \quad \frac{(1-c)}{1+\alpha^*\left(\frac{K_m}{K_c}-1\right)}=1 \tag{A1}$$

with

$$\alpha^*=\frac{1+\nu_c}{3(1-\nu_c)} \text{ and } \beta^*=\frac{2(4-5\nu_c)}{15(1-\nu_c)} \tag{A2}$$

$$\nu_c=\frac{1-\frac{2}{3}\left(\frac{\mu_c}{K_c}\right)}{2\left(1+\frac{1}{3}\frac{\mu_c}{K_c}\right)} \tag{A3}$$

for the case where the shear moduli and bulk moduli of the filler component are much larger than those of the matrix, as is the case for $CaCO_3$ and nylon. In the above equations c is the volume fraction of the filler component and μ_m and K_m are the shear and bulk moduli of the nylon. These simplified forms of the equations for the self consistent method provide very good estimates for $c < 0.3$. The method of Chow [18] which is in many respects more convenient in applications to filled polymers will give the following results.

$$\frac{K_c}{K_m}=1+\frac{\left(\frac{K_p}{K_m}-1\right)c}{1+\left(\frac{K_p}{K_m}-1\right)(1-c)\left(\frac{1+\nu_m}{1-\nu_m}\right)\frac{1}{3}} \tag{A4}$$

$$\frac{\mu_c}{\mu_m}=1+\frac{\left(\frac{\mu_p}{\mu_m}-1\right)c}{1+\left(\frac{\mu_p}{\mu_m}-1\right)\left[(1-c)\frac{1+\nu_p}{3(1-\nu_p)}+c\right]} \tag{A5}$$

where K_c and μ_c are the bulk and shear moduli of the filled blend, K_p and K_m are the bulk moduli of the $CaCO_3$ particles and the unmodified nylon, μ_p and the μ_m are, in turn, the shear moduli of the $CaCO_3$ particles and the unmodified nylon, c is the volume fraction of the particles. The Poisson's ratios of both the particles and the unmodified nylon in their free-standing form can be taken as 0.3 as a first approximation.

Once μ_c and K_c are determined the Young's modulus is obtained from the defining expression of

$$E_c=\frac{9K_c}{1+3K_c/\mu_c} \tag{A6}$$

for isotropic solids.

For the present application the shear modulus and bulk modulus of nylon was taken as $\mu_m = 646$ MPa, $K_m = 1.40$ GPa. Parantheticaly, the shear modulus and bulk

modulus of calcite are $\mu_p = 33.1$ GPa and $K_p = 67.1$ GPa as determined from Simmons and Wang [39]. Clearly, they are very much larger than those of nylon, lending support for the use of the simplified forms of the equations in the self consistent method given above.

Appendix B. The thermal misfit pressure between the $CaCO_3$ particles and the filled composite.

For the present case the thermal expansion misfit pressure in the spherical $CaCO_3$ particles arising from the thermal contraction of the filled nylon matrix around the particles is given by McClintock and Argon [19] as:

$$p = \frac{(\gamma_p - \gamma_c)\Delta T K_p}{\left[1 + \frac{4\mu_c}{3K_p}\right]} \tag{B1}$$

where γ_p and γ_c are the volumetric coefficients of expansion of the particles, and the filled composite. K_p is the bulk modulus of the particles and μ_c is the shear modulus of the filled nylon. The γ_c and μ_c themselves depend on the volume fraction c of particles and can be determined from the developments of Chow. Thus, we find from Chow [18,40]

$$\frac{\mu_c}{\mu_m} = 1 + \frac{\left(\frac{\mu_p}{\mu_m} - 1\right)c}{1 + \left[\left(\frac{\mu_p}{\mu_m} - 1\right)(1-c)\frac{2}{15}\frac{(4 - 5\nu_m)}{(1-\nu_m)}\right]} \tag{B2}$$

where ν_m is the Poisson's ratio of the nylon matrix which can be approximated by 0.3 and μ_m and μ_p are the shear moduli of the nylon matrix and the $CaCO_3$ particles respectively. Moreover, from Chow [40]

$$\gamma_p - \gamma_c = -\left(\frac{K_m}{K_p}\right)\frac{(\gamma_m - \gamma_p)c}{1 + \left(\frac{K_m}{K_p} - 1\right)\left[(1-c)\frac{1+\nu_p}{3(1-\nu_p)} + c\right]} \tag{B3}$$

where γ_c and γ_p are as stated above the volumetric coefficients of thermal expansion of the filled nylon and that of the particles respectively and K_m and K_p, are in turn the bulk moduli of nylon and $CaCO_3$. The Poisson's ratio of the particles ν_p can again be taken as 0.3.

Debonding in the form of a kink on the stress–strain curve will be observable when the negative pressure σ_m inside the particle, induced by the applied tensile stress equals the thermal-misfit-induced pressure to make the interfaces stress free and ready to undergo separation; where σ_m is obtainable from the classical work of Goodier [41] and is

$$p = \sigma_m = \frac{\sigma_{db}}{3}\left[1 + \frac{2(1 - 4\nu + \nu^2)\left(\frac{K_p}{K_c} - 1\right)}{(1+\nu)\left[2(1-2\nu) + (1+\nu)\left(\frac{K_p}{K_c}\right)\right]}\right] \tag{B4}$$

This gives eventually the tensile debonding stress σ_{db} as,

$$\sigma_{db} = \frac{3(\gamma_p - \gamma_c)\Delta T K_p}{\left(1 + \frac{4\mu_c}{3K_p}\right)} \times \left[1 + \frac{2(1 - 4\nu - \nu^2)\left(\frac{K_p}{K_c} - 1\right)}{(1+\nu)\left[2(1-2\nu) + (1+\nu)\frac{K_p}{K_c}\right]}\right]^{-1} \tag{B5}$$

where ν is the Poisson's ratio of the matrix which can again be taken as 0.3.

Appendix C. The essential work of fracture of matrix ligaments and the fracture toughness of filled polymers

As discussed in the text, strain hardening in semi-crystalline polymers involves crystallographic slip processes in the crystalline component where it results in texture development with a strong molecular alignment feature. In glassy polymers hardening involves a more diffuse process of molecular alignment which kinematically has a very close resemblance to similar processes in amorphous polymers above their glass transition and cross linked rubbers. In both cases the hardening component has a monotonically increasing plastic resistance as the aligned molecules become more and more directly load bearing.

Here for the purpose of developing a model for the essential work of fracture of matrix ligaments, identified in Section 4.5 as the representative volume elements between the debonded particles, we use the analytical formalisms of entropic rubber elasticity as stated e.g. by Boyce and Arruda [24]. When translated into a stretching resistive force f in the ligament, this formalism gives for uniaxial tension.

$$f = \frac{Y_0}{\lambda_1} + E_r G(\lambda_1, \lambda_n) \tag{C1}$$

where Y_0 is the temperature and strain rate dependent yield strength of the polymer, E_r the effective tensile (rubbery) hardening modulus, λ_1 the tensile extension ratio, λ_n, the terminal tensile 'locking' stretch and $G(\lambda_1, \lambda_n)$ a well established-albeit complicated function involving non-Gaussian statistics of incremental molecular segment alignment between cross links or molecular entanglements, characterized by the above two extension ratios. To a first approximation, the form of the second term on the RHS of Eq. (C1) is,

$$E_r G(\lambda_1, \lambda_n) \rightarrow \frac{3}{2}E_r(\lambda_1 - 1) \tag{C2}$$

between $\lambda_1 = 1$ and λ_n, where the resistive force is assumed to become unbounded. We emphasize again that the use of the above formalisms are for convenience in developing useful forms of expressions and does not represent advocacy of rubber elasticity as a mechanism to account for the strain

hardening behavior of a semi-crystalline polymer such as nylon.

The plastic work of ligament extension to final fracture when λ_1 reaches λ_n, where it is assumed that the rapidly rising deformation resistance will trigger wholesale chain scission, will take the form per unit thickness, in the limit where the first term in Eq. (C1) is dominant:

$$W_p \cong \frac{\pi d^2 Y_0}{4}\left(\frac{1-c}{c}\right)\ell n\lambda_n. \quad \text{(C3)}$$

Under impact conditions and at low temperatures where Y_0 increases significantly, chain scission in the stretched ligament will occur at extension ratios less than λ_n (see Section 4.8). From the above equation the essential work of fracture J_e is obtained directly as:

$$J_e = W_p/d(1+\Lambda/d) = \left(\frac{\sqrt{3}\pi}{8}\right)^{1/2}\left(\frac{1-c}{\sqrt{c}}\right)Y_0 d\,\ell n\lambda_n \quad \text{(C4)}$$

To determine the overall specific work of fracture or true fracture toughness J it is necessary to estimate the additional plastic work expanded in the crack flanks that accompanies the work of fracture J_e on the median plane of separation. As outlined in Section 4.5. This involves calculation of ΔJ from the gradient of local plastic ligament-stretch processes in the two process layers of thickness R_p where the ligament strain reduces down to the elastic strain at yield ϵ_0. Then

$$\Delta J = 2\int_{\delta}^{K_p}\frac{dJ}{dy}dy \quad \text{(C5)}$$

where

$$\frac{dJ}{dy} = 2Y_0(1-c)\epsilon(y) \quad \text{(C6a)}$$

and

$$\epsilon(y) \approx \frac{J}{Y_0 I_n y} \quad \text{(C6b)}$$

from the so-called HRR crack tip field relations for a non-hardening solid [42] where I_n is a definite integral in the HRR theory which drops out from our development. In Eq. (C5), δ is the half thickness of the layer inside which the central separation process of complete ligament rupture occurs. Thus, from Section 4.5 and the geometry of Fig. 27a,

$$\delta = \frac{\sqrt{3}}{4}d\left(\frac{\pi}{2\sqrt{3}c}\right)^{1/2} \quad \text{(C7)}$$

and

$$R_p = \delta\left(\frac{\epsilon_{fp}}{\epsilon_0}\right) = \delta\frac{\ell n_c}{\epsilon_0}. \quad \text{(C8)}$$

Evaluation of the integral in Eq. (C5) then gives, with the required substitutions:

$$J = 2\Delta J + J_e = J_e\left(1 + 2\,\ell n\left(\frac{\epsilon_{fp}}{\epsilon_0}\right)\right) \quad \text{(C9)}$$

where ϵ_{fp} the terminal fracture strain of the ligament is $\ell n\lambda_n$.

Appendix D. The triaxial tensile stress due to incomplete separation of particles

In reference to Fig. 30 we consider the incompletely separated particles as exerting a pressure on the walls of the spherical cavity (cylindrical in our 2-D model). An upper-bound estimate of this indentation pressure is taken to be βY_0, exerted along an arc length of αd of the periphery of the cavity wall, where we might take $\beta \approx 2$–3. Then the compressive forces F on the particles exerted by the matrix would be

$$F = \alpha d\beta Y_0 \quad \text{(D1)}$$

per unit thickness. Since no net lateral force is applied on the blend, beginning to deform plastically, there must be by equilibrium a compensating 2-D lateral (in-plane) negative pressure in the polymer matrix. This should then evoke a mean normal stress in the matrix of

$$\sigma_m = \frac{2\alpha\beta Y_0}{\sqrt{3}(1+(\Lambda/d))} = \alpha\beta\left(\frac{8c}{\sqrt{3}\pi}\right)^{1/2}Y_0. \quad \text{(D2)}$$

Taking $\alpha \approx 0.3$ and $\beta \approx 2.5$, the triaxial tensile stress that should be present at the early stages of ligament stretching is estimated to be $\sigma_m/Y_0 \approx 0.9c^{1/2}$.

References

[1] Lin J, Yee AF. Macromolecules 1988;31:7865.
[2] Argon AS, Bartczak Z, Cohen RE, Muratoğlu OK. Toughening of plastics: advances in modeling and experiments. In: Pearson RA, Sue HJ, Yee AF, editors. Modeling and experiments, Symposium Series 759. Washington, DC: ACS, 2000. p. 98.
[3] Qin J, Argon AS, Cohen RE. J Appl Polym Sci 1999;71:1469.
[4] Riew CK, Kinloch AJ, editors. Toughening of plastics II: novel approaches in science and engineering ACS Symposium Series 252. Washington, DC: ACS, 1996.
[5] Pearson RA, Sue H-J, Yee AF, editors. Toughening of plastics: advances in modeling and experiments ACS Symposium Series 759. Washington, DC: ACS, 2000.
[6] Wu SJ. J Appl Polym Sci 1998;35:549.
[7] Muratoğlu OK, Argon AS, Cohen RE. Polymer 1995;36:2143.
[8] Muratoğlu OK, Argon AS, Cohen RE, Weinberg M. Polymer 1995;36:921.
[9] Muratoğlu OK, Argon AS, Cohen RE, Weinberg M. Polymer 1995;36:4787.
[10] Bartczak Z, Argon AS, Cohen RE, Weinberg M. Polymer 1999;40:2331.
[11] Bartczak Z, Argon AS, Cohen RE, Weinberg M. Polymer 1999;40:2347.
[12] Galeski A, Argon AS, Cohen RE. Macromolecules 1988;21:2761.
[13] Peterlin AJ. Mater Sci 1971;6:490.
[14] Lin L, Argon AS. Macromolecules 1994;27:6903.
[15] Kumar V, German MD, Shih CF. An engineering approach for elastic–plastic fracture analysis, (NP-1931 research project 1237-1). Palo Alto, CA: Electric Power Research Institute, 1981.
[16] Muratoğlu OK, Argon AS, Cohen RE, Weinberg M. Polymer 1995;36:4771.

[17] Budiansky B. J Mech Phys Solids 1965;13:223.
[18] Chow TS. J Polym Sci (Polym Phys) 1978;16:959.
[19] McClintock FA, Argon AS. Mechanical behavior of materials. Reading, MA: Addison Wesley, 1966.
[20] Haward RN, Thackray G. Proc R Soc 1968;A302:453.
[21] Argon AS. Phil Mag 1973;28:839.
[22] Boyce MC, Parks DM, Argon AS. Mech Mater 1988;7:35.
[23] Boyce MC, Parks DM, Argon AS. Mech Mater 1988;7:15.
[24] Boyce MC, Arruda EM. Rubber Chem Technol 2000;73:504.
[25] Lee BJ, Argon AS, Parks DM, Ahzi S, Bartczak Z. Polymer 1993;34:3555.
[26] Ahzi S, Lee BJ, Asaro RJ. Mater Sci Engng 1994;A189:35.
[27] Galeski A, Argon AS, Cohen RE. Macromolecules 1991;24:3953.
[28] Pflüger R. In: Brandrup J, Immergut EH, editors. Polymer handbook, 3rd ed. New York: Wiley, 1989.
[29] Danielsson M, Parks DM, Boyce MC. Submitted for publication.
[30] Tzika PA, Boyce MC, Parks DM. J Mech Phys Solids 2000;48:1893.
[31] Qin J, Argon AS, Cohen RE. J Appl Polym Sci 1999;71:1469.
[32] Zhurkov SN, Kuksenko VS, Slutsker AI. In: Pratt PL, editor. Fracture 1969. London: Chapman and Hall, 1969. p. 531.
[33] Peterlin A. J Macromol Sci Phys 1973;B*(1-2):83.
[34] Tunca C, Argon AS, Cohen RE. To be published.
[35] Muratoğlu OK, Argon AS, Cohen RE, Weinberg M. Polymer 2001, in press.
[36] Argon AS. In: Kelly A, Zweben C, editors. Comprehensive composite materials, Amsterdam: Elsevier, 2000. p. 763, Chap. 24 (edited by Chou TW).
[37] Bartczak Z, Argon AS, Cohen RE, Kowalewski B. Polymer 1999;40:2367.
[38] deHoff RT, Rhines FN. Quantitative microscopy. New York: McGraw-Hill, 1968.
[39] Simmons G, Wang H. Single crystal elastic constants and calculated aggregate properties: a handbook. Cambridge, MA: MIT Press, 1971.
[40] Chow TS. J Polym Sci (Polym Phys) 1978;16:967.
[41] Goodier JN. ASME Trans 1933;55:39.
[42] Hutchinson JW. J Mech Phys Solids 1968;16:13.